

COLLIDING HOLES IN RIEMANN SURFACES AND QUANTUM CLUSTER ALGEBRAS

LEONID CHEKHOV* AND MARTA MAZZOCCO†

ABSTRACT. We investigate *bordered cusped Teichmüller spaces*, which are Teichmüller spaces of Riemann surfaces with at least one hole and at least one *bordered cusp* on its boundary. We propose a combinatorial graph description of this bordered cusped Teichmüller space and endow it with a Poisson structure, quantization of which can be achieved with a canonical quantum ordering. We show how cusped Riemann surfaces arise when colliding holes in a Riemann surface. In the limit of two colliding holes (or colliding sides of the same hole), the geodesics that originally passed through the domain between colliding holes, which we call *chewing-gum*, become geodesic arcs between two bordered cusps decorated by horocycles. The lengths of these arcs are λ -lengths in Thurston–Penner terminology, or cluster variables by Fomin and Zelevinsky. We then consider classes of geodesic laminations comprising both closed curves in the interior of a Riemann surface and arcs passing between bordered cusps. We find the Poisson and quantum algebras of these laminations. We introduce an extended set of shear coordinates (Y -variables in cluster terminology) on Riemann surfaces with holes/orbifold points and decorated bordered cusps. We demonstrate that for any Riemann surface $\Sigma_{g,s,n}$ of genus g with $s \geq 1$ holes/orbifold points and $n \geq 1$ bordered cusps, we have geodesic laminations that are complete systems of arcs, or λ -lengths, or X -cluster variables together with closed paths (ω -cycles) around holes without bordered cusps or around orbifold points. (Every such system of arcs and ω -cycles comprises exactly $6g - 6 + 3s + 2n$ elements and corresponds to a seed of a cluster.) We construct an explicit 1-1 relation between these variables and the extended shear coordinates and use the invariance under quantum flip morphisms to prove that the homogeneous q -commutation relations on the set of extended shear coordinates imply homogeneous q -commutation relations between arcs in the same seed (which therefore corresponds to a quantum torus). As a byproduct, we solve the problem of quantum ordering of shear coordinates in expressions for arcs and give an explicit combinatorial proof of the Laurent and positivity properties of X -cluster variables in any seed. From the physical point of view, our construction provides an explicit coordinatization of moduli spaces of open/closed string worldsheets and their quantization.

1. INTRODUCTION

In this paper, we investigate Riemann surfaces containing *bordered cusps* on their boundary components. In Poincaré uniformisation, these cusps correspond to ideal triangles in the fundamental domain. We call *bordered cusped Riemann surface* a Riemann surface $\Sigma_{g,s,n}$ of genus g with $s \geq 1$ holes or orbifold points and with additional $n \geq 1$ *bordered cusps* situated on holes to which these cusps are assigned. We introduce the notion of *bordered cusped Teichmüller space* generalising the shear coordinates and the geodesic length functions to this case, and we give a complete set of coordinates on it for which the Goldman bracket is closed.

Finding Darboux coordinates (quantum tori) for the moduli spaces of Riemann surfaces is important for solving many problems of theoretical physics. Such coordinates for moduli spaces of Riemann surfaces with holes were identified in [6] with the shear coordinates for an ideal triangle decomposition obtained in [19] by generalising the results for punctured Riemann surfaces proved in [45]. In this paper, we introduce the Teichmüller spaces $\widehat{\mathfrak{T}}_{g,s,n}$ of $\Sigma_{g,s,n}$ and we provide a full coordinatization for them in terms of extended shear coordinates.

*Steklov Mathematical Institute of Russian Academy of Sciences, Moscow, Russia; Email: chekhov@mi.ras.ru.

†Department of Mathematical Sciences, Loughborough University, LE11 3TU, United Kingdom. Email: m.mazzocco@lboro.ac.uk.

In physical terms, we provide an explicit coordinatization of open/closed string worlsheds described as *windowed surfaces* by R. Kaufmann and Penner in [34] where they considered laminations of Riemann surfaces $\Sigma_{g,s,n}^w$ of genus g with $s > 0$ holes (boundary components) and with $n \geq 0$ *windows* that were domains stretched between marked points located on the boundaries of the holes. These laminations comprised both closed curves and curves starting and terminating at windows thus describing foliations of $\Sigma_{g,s,n}^w$. In our construction, we decorate $\Sigma_{g,s,n}$ by horocycles based at the endpoints of the bordered cusps; laminations on the windowed surfaces $\Sigma_{g,s,n}^w$ then correspond to sets of arcs stretched between bordered cusps, so, literally, windows of Kaufmann and Penner are segments of horocycles confined between two bordering geodesic curves separating windows. In the present paper, we describe the Teichmüller spaces $\widehat{\mathfrak{T}}_{g,s,n}$ of $\Sigma_{g,s,n}$; the Kaufmann–Penner coordinates on the space of laminations are then the projective (tropical) limit of the extended shear coordinates $\{Z_\alpha, \pi_j\}$ on $\widehat{\mathfrak{T}}_{g,s,n}$ introduced in this paper. We thus provide a convenient parameterization of the open/closed string worlsheds and their quantization.

The main objects describing Riemann surfaces in a mapping-class-group-invariant way are *geodesic functions*—double hyperbolic cosines of half-lengths of closed geodesics. Geodesic functions customarily constitute sets of observables; in the classical case, the set of geodesic functions is often called the *spectrum of a Riemann surface*. Upon quantisation, the observables of a quantum Riemann surface are given by an algebra of quantum geodesic functions. An explicit combinatorial construction of the corresponding classical geodesic functions in terms of shear coordinates of decorated Teichmüller spaces for Riemann surfaces with holes was proposed in [7]: it was shown there that all geodesic functions are Laurent polynomials of exponentiated coordinates with positive integer coefficients; this remains true for Riemann surfaces with \mathbb{Z}_2 and \mathbb{Z}_3 orbifold points [4], [5]; the integrality condition breaks in general in the case of orbifold points of arbitrary order [14] but positivity remains in this case as well. In [14], a general combinatorial construction of geodesic functions in terms of shear coordinates for orbifold Riemann surfaces was constructed, as a byproduct of this constructions, new generalised cluster transformations (cluster algebras with coefficients) were introduced.

However the problem of producing a closed Poisson algebra of geodesic functions on a Riemann surface $\Sigma_{g,s}$ for any genus g and any number $s_h > 1$ of holes and any number of s_o of orbifold points remained open (here $s = s_o + s_h$). In this paper we fully characterise the Poisson algebra of geodesic functions on $\Sigma_{g,s}$ as a specific Poisson sub-algebra of the set of geodesics functions and *arcs* on $\Sigma_{g,s,1}$, i.e. a Riemann surface of genus g with at least one hole and one *bordered cusp* on the boundary (see Subsection 4.8).

Let us describe the origin of our bordered cusps: they naturally appear (with decorations by horocycles) from colliding two holes or two sides of the same hole in a Riemann surface. In this situation, we obtain an infinitely thin and infinitely long (in metric sense) domain, called *chewing-gum*. We regularise this chewing-gum by introducing some “collars” and subtracting the infinite parts between these collars. Upon taking the limit to infinity, the chewing gum breaks into two bordered cusps and the collars become horocycles decorating these cusps on the newly obtained Riemann surface. Geodesics that were passing along the chewing gum become *arcs* – infinitely long geodesics that start and terminate at bordered cusps – and the parts of geodesics stretched between collars in the rest of the Riemann surface become arcs between decorating horocycles, so that the geodesic length—functions become, genuine λ lengths in the Penner–Thurston description.

We also attack the problem of quantum ordering of the product of non-commuting operators obtained by quantising this picture. This is customarily among the most subtle issues of quantum mechanics and quantum field theory.

Shear coordinates were quantized in [6] and in the Liouville-type parameterisation in [32]. Universally, the quantum mapping-class group (MCG) transformations (or, the quantum flip morphisms) that satisfy the quantum pentagon identity were based on the quantum dilogarithm function [18]. Shear coordinates can be identified with the Y -type cluster variables [26], [28].

As regarding quantum geodesic functions, this problem was first mentioned in [7] where the determining conditions of mapping-class-group (MCG) invariance and satisfaction of the quantum skein relations were formulated. The compatibility of these two conditions was implicitly proved by Kashaev [33] who constructed unitary operators of quantum Dehn twists whose action on operators of quantum geodesic functions obviously preserves their quantum algebra. It remained however the problem of formulating a recipe for obtaining a quantum operator in an explicit form, likewise the Kulish, Sklyanin, and Nazarov recipe (see [35], [43]) for constructing Yangian central elements extended to the case of twisted Yangians by Molev, Ragoucy, and Sorba (the quantum ordering for twisted Yangians was constructed in [38] for the $O(n)$ case and in [39] for the $Sp(2n)$ case).

In this paper we solve the problem of quantum ordering by introducing the notion of *cusped geodesic lamination* (CGL) comprising both closed geodesic lines and arcs such that elements of a CGL have no intersections nor self-intersections in the interior of a Riemann surface, but arcs from the same CGL can be incident to the same bordered cusp (note that this condition establishes a linear ordering on the set of ends of arcs belonging to the same CGL and incident to the same bordered cusp). The corresponding algebraic objects are $\prod_{\gamma \in \text{CGL}} (2 \cosh(l_\gamma/2)) \prod_{\mathbf{a} \in \text{CGL}} e^{l_{\mathbf{a}}/2}$ where l_γ are geodesic lengths of the corresponding closed geodesics γ and $l_{\mathbf{a}}$ are signed lengths of the parts of arcs \mathbf{a} between two horocycles decorating the corresponding cusps. The combination $2 \cosh(l_\gamma/2)$ is customarily called the geodesic function being the trace of the corresponding element of a Fuchsian group. By analogy, we call $e^{l_{\mathbf{a}}/2}$ the arc function, or λ -length. We prove the following theorem:

Theorem. For any Riemann surface $\Sigma_{g,s,n}$ of genus g with $s_h \geq 1$ holes, s_o orbifold points, $s = s_o + s_h$, and with $n \geq 1$ bordered cusps, there always exists a maximum CGLs denoted by $\text{CGL}_{\mathbf{a}}^{\max}$ that comprises exactly $6g - 6 + 3s + 2n - n_o$ elements that are arcs and ω -cycles (closed loops around holes not containing bordered cusps). Arcs from $\text{CGL}_{\mathbf{a}}^{\max}$ are edges of an ideal triangle partition of $\Sigma_{g,s,n}$ in which every hole that does not contain bordered cusps and every orbifold point is enclosed in a monogon. Moreover the λ -lengths of the arcs in $\text{CGL}_{\mathbf{a}}^{\max}$ satisfy homogeneous Poisson brackets and their quantisation satisfy homogeneous commutation relations (see formulae (4.18), (5.22)).

We introduce extended shear coordinates $\{Z_\alpha, \pi_j\}$ of a graph $\widehat{\mathcal{G}}$ that is a spine of $\Sigma_{g,s,n}$ ($n \geq 1$) in which all holes without bordered cusps and all orbifold points are contained in loops, at every bordered cusp we have exactly one one-valent vertex, and all other vertices are three-valent.

We describe explicitly the 1 : 1 correspondence between these extended shear coordinates and λ -lengths (exponentiated signed half-lengths of parts of arcs confined between horocycles) of arcs in the $\text{CGL}_{\mathbf{a}}^{\max}$ corresponding to the ideal triangle partition dual to this $\widehat{\mathcal{G}}$. In this correspondence, every loop in $\widehat{\mathcal{G}}$ corresponds to either an ω -cycle or to an orbifold point in $\text{CGL}_{\mathbf{a}}^{\max}$ containing the same hole/orbifold point. The edge of $\widehat{\mathcal{G}}$ incident to a loop corresponds to the arc bordering a monogon from $\text{CGL}_{\mathbf{a}}^{\max}$, every edge of $\widehat{\mathcal{G}}$ joining two different three-valent vertices intersects with exactly one arc of $\text{CGL}_{\mathbf{a}}^{\max}$, and every edge of $\widehat{\mathcal{G}}$ terminating at a bordered cusp corresponds to the bordering arc immediately to the left of this cusp.

The two Poisson and quantum algebras of $\{Z_\alpha, \pi_j\}$ and of arc functions in $\text{CGL}_{\mathbf{a}}^{\max}$ therefore imply one another and we prove that quantum algebras of arc functions from the same $\text{CGL}_{\mathbf{a}}^{\max}$ satisfy the same quantum commutation relations as in the quantum cluster algebras by Berenstein–Zelevinsky [2]. We can therefore identify a $\text{CGL}_{\mathbf{a}}^{\max}$ with a seed of a quantum cluster algebra in such a way that the quantum cluster algebras we obtain - let us call them *quantum cluster algebras of geometric type* - satisfy the main axioms of the Berenstein–Zelevinsky construction. However, the mutation transformations in our quantum cluster algebras of geometric type include also generalized cluster transformations from [14] besides the standard Ptolemy-type mutations. Moreover, the Laurent and positivity properties for geodesic functions expressed in the extended shear coordinates directly imply the Laurent and positivity properties for our quantum cluster algebras of geometric type. It is interesting to mention that in the case of the bordered cusped Teichmüller spaces $\mathcal{T}_{g,s,n}$ with $n \geq 1$ both

the extended shear coordinates and λ -lengths of arcs from a $\text{CGL}_{\mathfrak{a}}^{\max}$ of $\Sigma_{g,s,n}$ satisfy homogeneous q -commutation relations being therefore quantum tori. The price for the existence of Poisson and quantum algebras of λ -lengths in our case is that we do not consider arcs starting and/or terminating at punctures (holes), that is, we completely avoid the issue of tagging [25], [24].

For any given $\text{CGL}_{\mathfrak{a}}^{\max}$ of the above type, we have the dual fat graph for which (see Proposition 4.1) all λ -lengths of arcs from this lamination are monomials in $e^{Z_{\alpha}/2}$, $e^{\pi_j/2}$ and, vice versa, all $e^{Z_{\alpha}/2}$, $e^{\pi_j/2}$ are monomials in $\lambda_{\mathfrak{a}}^{\pm 1/2}$.

The case of $g = 0$ and $2s + n \geq 8$ is treated in great detail in [12] due to its links with the theory of the Painlevé differential equations. It is interesting to observe that in these cases the chewing gum moves produce the confluence scheme of the Painlevé differential equations, and at quantum level it produces the confluence of the spherical sub-algebras of the confluent Cherednik algebras defined in [36]. The role of cluster algebras in the Cherednik algebra setting will be investigated further in subsequent publications.

We remark that a quantitative description of surfaces with bordered cusps could be deduced from works by Fock and Goncharov [20], Musiker, Schiffler and Williams [40], [42], and S. Fomin, M. Shapiro, and D. Thurston [25], [24]. In particular the authors of [25] considered systems of (tagged) arcs starting and terminating either at bordered cusps or at punctures (holes) of $\Sigma_{g,s,n}$. Due to the satisfaction of the Ptolemy relations for λ -lengths of arcs [45], the correspondence to cluster algebras was immediate; in [40] the positivity property for λ -lengths of arcs connecting marked points (bordered cusps in our terminology) was proved in a technically rather elaborated way with the use of Ptolemy relations only. Then, in [42], a nice quantitative description of simple arcs was attained: their λ -lengths were identified with upper-right elements (denoted K -traces in the present text) of products of 2×2 -matrices from $PSL(2, \mathbb{R})$ and a part of skein relations between these elements were constructed (Lemma 6.11 of [42]).^a

The structure of the paper is as follows. In Sec. 2, we present some known facts about quantum geodesics, quantum MCG transformations, and quantum ordering for shear coordinates and λ -lengths.

The new material starts in Sec. 3 with the geometrical picture in Poincaré geometry in which we consider colliding holes visualised as a “chewing gum” construction. We prove that in the limit of broken chewing gum we obtain the Ptolemy relations for arc functions of the newly obtained arcs out of skein relations satisfied by the geodesic functions before taking the limit.

In Sec. 4 we define the *bordered cusped Teichmüller spaces* of bordered cusped Riemann surfaces and provide the explicit fat-graph (combinatorial) description of arcs (and, therefore, for λ -lengths and for the corresponding X -cluster variables) in terms of the extended set of shear coordinates of the new Riemann surface with decorated bordered cusps. We consider cusped geodesic laminations CGL that are collections of closed geodesics $\gamma \in \text{CGL}$ and arcs $\mathfrak{a} \in \text{CGL}$ such that entries of a geodesic lamination have no (self)intersections inside the Riemann surface, but different arcs can be incident to the same bordered cusp, and introduce the corresponding algebraic objects. We explicitly write the 1-1 correspondence between arc functions of arcs from a $\text{CGL}_{\mathfrak{a}}^{\max}$ and extended shear coordinates of the fat graph dual to this lamination. We also describe how the Kauffmann–Penner coordinatized lamination space of windowed Riemann surfaces appear as a projective limit of our λ -length description and compare our approach with that of Fomin, M. Shapiro, and D. Thurston (see [25, 24]). We conclude this section with the description of Poisson algebras of arc functions proving that arc functions from the same CGL have homogeneous Poisson brackets.

In Sec. 5, we formulate the quantum MCG transformations for shear coordinates and the quantum mutations for arcs for Riemann surfaces with bordered cusps and find quantum commutation relations between the new shear coordinates that are invariant w.r.t. these MCG transformations. For arcs, we explicitly construct the quantum ordering that is invariant under the action of the quantum MCG. This

^aCuriously, a missed relation in [42] was just the Ptolemy relation: following the authors of [42], let $ur(M)$ denote the upper-right element of the matrix M , then, for any four (2×2) -matrices M_i with unit determinants, $ur(M_1 M_2) ur(M_3 M_4) = ur(M_1 M_4) ur(M_3 M_2) + ur(M_1 M_3^{-1}) ur(M_2^{-1} M_4)$.

quantum ordering coincides with the natural ordering. The quantum commutation relations between arc functions from the same CGL become homogeneous thus defining a quantum torus. We then write quantum mutation relations induced by quantum MCG transformations exclusively in terms of quantum λ -lengths of arcs from the same CGL_a^{\max} . We can therefore identify any CGL_a^{\max} with a *seed* of a Berenstein–Zelevinsky quantum cluster algebra [2]; these seeds are related by quantum mutations, which include besides the standard binomial terms also terms corresponding to generalized cluster transformations. We thus provide a geometric setting for the quantum cluster algebras.

2. IMPORTANT FACTS ON QUANTUM GEODESICS, QUANTUM TEICHMÜLLER SPACES, AND RELATED λ -LENGTHS (CLUSTER VARIABLES)

In this section, we briefly recall the combinatorial construction of Riemann surfaces with holes and orbifold points from [45, 19, 32, 6, 7, 14, 10] with some slight adaptations which are useful in this paper.

2.1. Combinatorial description of $\mathfrak{T}_{g,s}^H$. We first describe the relation between fat graphs endowed with elements of $PSL(2, \mathbb{R})$ and Fuchsian groups.

2.1.1. Fat graph description for Riemann surfaces with holes and \mathbb{Z}_p orbifold points.

Definition 2.1. We call a fat graph (a graph with the prescribed cyclic ordering of edges entering each vertex) \mathcal{G}_{g,s_h,s_o} a *spine of the Riemann surface* Σ_{g,s_h,s_o} with g handles, $s_h > 0$ holes, and s_o orbifold points of the corresponding orders p_i , $i = 1, \dots, s_o$, if

- (a) this graph can be embedded without self-intersections in Σ_{g,s_h,s_o} ;
- (b) all vertices of \mathcal{G}_{g,s_h,s_o} are three-valent;
- (c) upon cutting along all edges of \mathcal{G}_{g,s_h,s_o} the Riemann surface Σ_{g,s_h,s_o} splits into $s = s_h + s_o$ polygons each containing exactly one hole or an orbifold point and being simply connected upon contracting this hole or removing the orbifold point. All polygons containing orbifold points (and some, but not all polygons containing holes) are monogons, that is, every such monogon is bounded by an edge that starts and terminates at the same three-valent vertex of the spine.

Remark 2.2. In our previous papers, we considered a situation with “pending” edges corresponding to orbifold points. In this paper instead, we attach additional loops to ends of these edges. This enables us treating holes and orbifold points on the equal footing, so we often write $\mathcal{G}_{g,s}$ and $\Sigma_{g,s}$ with $s = s_h + s_o$ without distinguishing between holes and orbifold points.

The edges in the above graph are labeled by distinct integers $\alpha = 1, 2, \dots, 6g - 6 + 3s$, and we set a real number Z_α into correspondence to the α th edge if it is not a loop. To each edge that is a loop we set into correspondence the number ω_i such that

$$(2.1) \quad \omega_i = \begin{cases} 2 \cosh(P_i/2) & \text{if the monogon contains a hole with the perimeter } P_i \geq 0, \\ 2 \cos(\pi/p_i) & \text{if the monogon contains an orbifold point of order } p_i \in \mathbb{Z}_+, p_i \geq 2. \end{cases}$$

The first homotopy groups $\pi_1(\Sigma_{g,s_h,s_o})$ and $\pi_1(\mathcal{G}_{g,s_h,s_o})$ coincide because each closed path in Σ_{g,s_h,s_o} can be homotopically transformed to a closed path in \mathcal{G}_{g,s_h,s_o} (taking into account paths that go around orbifold points) in a unique way. The standard statement in hyperbolic geometry is that conjugacy classes of hyperbolic elements of a Fuchsian group $\Delta_{g,s_h,s_o} \subset PSL(2, \mathbb{R})$ are in the 1-1 correspondence with homotopy classes of closed paths in the Riemann surface $\Sigma_{g,s_h,s_o} = \mathbb{H}_+^2 / \Delta_{g,s_h,s_o}$ so that we can refer to the length ℓ_γ of a hyperbolic element $\gamma \in \Delta_{g,s_h,s_o}$ to mean the minimum length of curves from the corresponding homotopy class; it is then the length of a unique closed geodesic line belonging to this class.

The real numbers Z_α in Definition 2.1 are the h -lengths (logarithms of cross-ratios) [45]: they are called the (*Thurston*) *shear coordinates* [46],[3] in the case of punctured Riemann surface (when all

$P_i = 0$). We identify these shear coordinates with coordinates of the decorated Teichmüller space $\mathfrak{T}_{g,s_h,s_o}^H$. It was proved in [14] that any metrizable Riemann surface of genus g with exactly s_o orbifold points of the prescribed orders p_i and s_h holes with the prescribed perimeters P_i corresponds, up to the action of a discretely acting MCG group, to a fat graph \mathcal{G}_{g,s_h,s_o} whose edges are endowed with the real numbers Z_α and ω_i and, vice versa, for any choice of the above real numbers we have a metrizable Riemann surface corresponding to such fat graph. The correspondence is understood as the coincidence of *spectra* of the above objects: the sets of lengths of closed geodesics (geodesic functions) on the Riemann surface and on the graph.

In the case of surfaces with punctures, the dual to the above fat graph description is an *ideal triangle decomposition* constructed in [45]. This description was generalised to surfaces with holes in [19] and to surfaces with holes and orbifold points in [4, 5, 14]. Each edge of a dual graph (a side of an ideal triangle decorated by horocycles based at its vertices) carries a λ length, which is by definition

$$(2.2) \quad \lambda_\alpha = e^{l_\alpha/2}$$

where l_α is the signed length of the part of the ideal triangle edge confined between two horocycles based at the ends of this edge (the sign is negative if these horocycles intersect)^b. The mapping class group acts on the set of lambda lengths by morphisms, which are dual to those for h -lengths and correspond to mutations of cluster variables, which results in a natural identification of lambda lengths with a subclass of cluster varieties of a geometrical origin in [28].

The h -lengths are related to the λ -lengths through the cross-ratio relation (see the left-hand side of Fig. 3)

$$(2.3) \quad e^{Z_e} = \frac{\lambda_b \lambda_d}{\lambda_a \lambda_c}.$$

The geometrical meaning of Z_e is the signed geodesic distance between perpendiculars to the common side e of two adjacent ideal triangles through the vertices of these triangles (see examples in Fig. 3).

2.1.2. The Fuchsian group Δ_{g,s_h,s_o} and geodesic functions. The combinatorial description of conjugacy classes of the Fuchsian group Δ_{g,s_h,s_o} is attained in terms of (closed) paths on \mathcal{G}_{g,s_h,s_o} to which we set into correspondence products of matrices from $PSL(2, \mathbb{R})$. Every time the path homeomorphic to a (closed) geodesic γ passes along the edge with the label α we insert [19] the so-called *edge matrix*:

$$(2.4) \quad X_{Z_\alpha} = \begin{pmatrix} 0 & -e^{Z_\alpha/2} \\ e^{-Z_\alpha/2} & 0 \end{pmatrix}$$

into the corresponding string of matrices. We also have the “right” and “left” turn matrices to be set in proper places when a path makes corresponding turns at three-valent vertices (except those incident to loops),

$$(2.5) \quad R = \begin{pmatrix} 1 & 1 \\ -1 & 0 \end{pmatrix}, \quad L = R^2 = \begin{pmatrix} 0 & 1 \\ -1 & -1 \end{pmatrix}.$$

When orbifold points are present, the Fuchsian group contains besides hyperbolic elements also elliptic elements corresponding to rotations about these orbifold points. The corresponding generators \tilde{F}_i , $i = 1, \dots, s_o$, of the rotations through $2\pi/p_i$ are conjugates of the matrices F_{ω_i} ,

$$(2.6) \quad \tilde{F}_i = U_i F_{\omega_i} U_i^{-1}, \quad F_{\omega_i} := \begin{pmatrix} 0 & 1 \\ -1 & -\omega_i \end{pmatrix}, \quad \omega_i = 2 \cos(\pi/p_i).$$

Following [14], we introduce special matrices corresponding to going along a loop labeled by ω_i (2.1) (without differing between orbifold points and holes contained inside the loop): every time a path goes clockwise around the loop (see Fig. 1(a)), we insert the matrix (2.6) in the corresponding string of

^bWe remind the reader that in this approach the choice of a horocycle at each vertex of the ideal triangulation is fixed once for ever and that the Euclidean diameters of such horocycles constitute the “decoration” in [45].

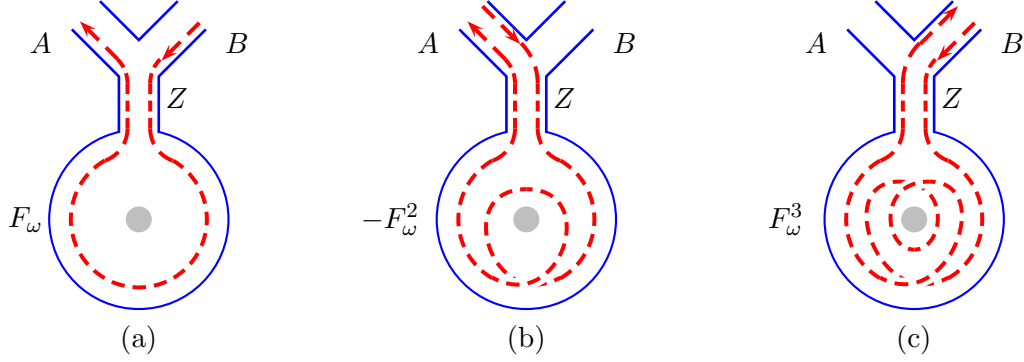


FIGURE 1. Part of a graph with a loop. The variable Z corresponds to a unique edge incident to the loop. We present three typical examples of geodesics undergoing single (a), double (b), and triple (c) clockwise rotations.

matrices (*without* adding the matrices of left/right turns, i.e., the corresponding string has the form $\cdots X_{Z_\alpha} F_{\omega_i} X_{Z_\alpha} \cdots$, where α is the label of the unique edge attached to the loop). When going along a loop k times clockwise we insert the matrix $(-1)^{k+1} F_\omega^k$ into the product of 2×2 -matrices. For example, parts of geodesic functions in the three cases in Fig. 1 where we denote the shear coordinates by A, B, Z , read:

$$\begin{aligned}
 (2.7) \quad & \text{(a)} \quad \cdots X_A L X_Z F_\omega X_Z L X_B \cdots, \\
 & \text{(b)} \quad \cdots X_A L X_Z (-F_\omega^2) X_Z R X_A \cdots, \\
 & \text{(c)} \quad \cdots X_B R X_Z (F_\omega^3) X_Z L X_B \cdots.
 \end{aligned}$$

Note that $F_{\omega_p}^p = (-1)^{p-1} \mathbb{E}$ when $\omega_p = 2 \cos \pi/p$, so going around the \mathbb{Z}_p orbifold point p times merely corresponds to avoiding this loop. (For the \mathbb{Z}_2 orbifold points this pattern was first proposed by Fock and Goncharov [21]; the graph morphisms were described in [5].)

If a loop circumnavigates a hole, not an orbifold point, then, when going around it counterclockwise, we must insert the matrix $-F_\omega^{-1} = \begin{pmatrix} w & 1 \\ -1 & 0 \end{pmatrix}$, etc.

As explained in Remark 2.2, this convention saves us from distinguishing between holes and orbifold points in all our computations. To revert to the usual setting in which the portion of the geodesic going clockwise around the loop like Fig. 1(a) is described by $X_Z L X_P L X_Z$ rather than by $X_Z F_\omega X_Z$, we just need to shift the shear coordinate Z by $P/2$. In other words,

$$X_Z L X_P L X_Z = X_{Z+P/2} F_\omega X_{Z+P/2}.$$

Resuming, an element P_γ in the Fuchsian group has then the typical structure:

$$(2.8) \quad P_\gamma = L X_{Z_n} R X_{Z_{n-1}} \cdots R X_{Z_{j+1}} L X_{Z_j} (-1)^{k+1} F_{\omega_i}^k X_{Z_{j-1}} R \cdots X_{Z_1}.$$

In the corresponding *geodesic function*

$$(2.9) \quad G_\gamma \equiv \text{tr } P_\gamma = 2 \cosh(\ell_\gamma/2),$$

ℓ_γ is the actual length of the closed geodesic on the Riemann surface.

Remark 2.3. Note that the combinations

$$\begin{aligned} RX_Z &= \begin{pmatrix} e^{-Z/2} & -e^{Z/2} \\ 0 & e^{Z/2} \end{pmatrix}, \quad LX_Z = \begin{pmatrix} e^{-Z/2} & 0 \\ -e^{-Z/2} & e^{Z/2} \end{pmatrix}, \\ RX_Z F_\omega X_Z &= \begin{pmatrix} e^{-Z} + \omega & -e^Z \\ -\omega & e^Z \end{pmatrix}, \quad LX_Z F_\omega X_Z = \begin{pmatrix} e^{-Z} & 0 \\ -e^{-Z} - \omega & e^Z \end{pmatrix}, \\ RX_Z(-F_\omega^{-1})X_Z &= \begin{pmatrix} e^{-Z} & -e^Z - \omega \\ 0 & e^Z \end{pmatrix}, \quad LX_Z(-F_\omega^{-1})X_Z = \begin{pmatrix} e^{-Z} & -\omega \\ -e^{-Z} & e^Z + \omega \end{pmatrix}, \end{aligned}$$

as well as products of any number of these matrices have the sign structure $\begin{pmatrix} + & - \\ - & + \end{pmatrix}$, so the trace of any element P_γ with first powers of F_ω and/or $-F_\omega^{-1}$ is a sum of exponentials with positive integer coefficients. This observation will be important when proving positivity of cluster transformations in Sec. 4.

The group generated by elliptic elements (2.6) together with hyperbolic elements corresponding to translations along A - and B -cycles of the Riemann surface and around holes is not necessarily Fuchsian because its action may not be discrete. The necessary and sufficient conditions under which we obtain a *regular* (that is, locally smooth everywhere except exactly s_o orbifold points) Riemann surface were formulated in terms of graphs in [14] where it was proven that we obtain a regular Riemann surface for any set of real numbers Z_α from Definition 2.1 and vice versa. For a given Riemann surface, this set is not unique and equivalent sets are related by discrete modular group action, so we identify the $(6g - 6 + 3s_h + 2s_o)$ -tuple of real coordinates $\{Z_\alpha\}$ with the coordinates of the decorated Teichmüller space $\mathfrak{T}_{g,s_h,s_o}^H$ (the decoration assigns positive or negative signs to every hole with nonzero perimeter). The lengths of geodesics on Σ_{g,s_h,s_o} are given by traces of products (2.8) corresponding to paths in the corresponding spine.

Transitions between different parameterizations are formulated in terms of flip morphisms (mutations) of edges: any two spines from the given topological class are related by a finite sequence of flips. We therefore identify flips on edges with the MCG action.

2.2. Poisson structure. One of the most attractive properties of the graph description is a very simple Poisson algebra on the set of coordinates Z_α , $\alpha = 1, \dots, 6g - 6 + 3s_h + 2s_o$.

Theorem 2.1. *In the coordinates Z_α on any fixed spine corresponding to a surface with or without orbifold points, the Weil–Petersson bracket B_{WP} reads*

$$(2.10) \quad \{f(\mathbf{Z}), g(\mathbf{Z})\} = \sum_{\substack{\text{3-valent} \\ \text{vertices } \alpha = 1}}^{4g+2s+|\delta|-4} \sum_{i=1}^{3 \bmod 3} \left(\frac{\partial f}{\partial Z_{\alpha_i}} \frac{\partial g}{\partial Z_{\alpha_{i+1}}} - \frac{\partial g}{\partial Z_{\alpha_i}} \frac{\partial f}{\partial Z_{\alpha_{i+1}}} \right),$$

where the sum ranges all three-valent vertices of a graph and α_i are the labels of the cyclically (clockwise) ordered ($\alpha_4 \equiv \alpha_1$) edges incident to the vertex with the label α . This bracket gives rise to the Goldman bracket on the space of geodesic length functions [31].

Note that formula (2.10) is insensitive to whether we include or remove vertices incident to loops into this sum because the term in brackets is identically zero for such a vertex. The quantities ω_i are therefore central and we interpret them as parameters.

The center of the Poisson algebra (2.10) is generated by elements of the form $\sum Z_\alpha$, where the sum ranges all edges of \mathcal{G}_{g,s_h,s_o} (taken with multiplicities) belonging to the same boundary component (which can also be a monogon containing a hole). The dimension of this center is obviously s_h .

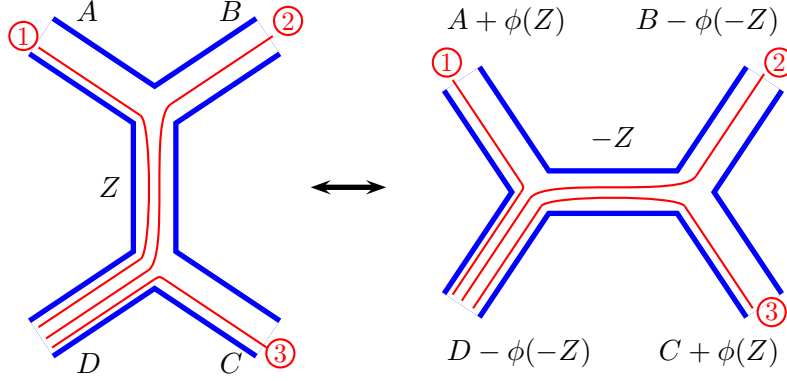


FIGURE 2. Flip on the shear coordinates Z_α . The edge undergoing the flip is assumed to be an internal edge that is neither a loop nor adjacent to a loop. We indicate the correspondences between geodesic paths undergoing the flip.

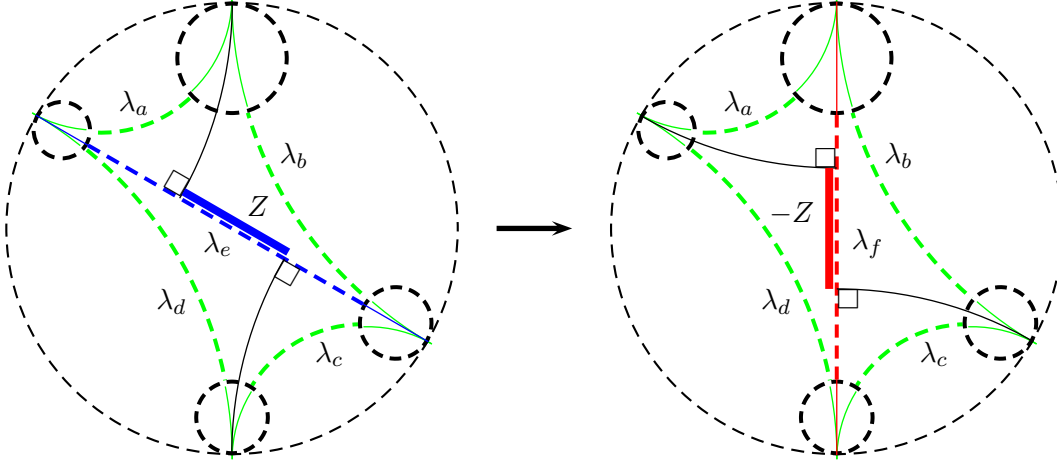


FIGURE 3. The transformation dual to the flip in Fig. 2: the flip, or mutation transformation, for the λ -lengths subject to the Ptolemy relation $\lambda_e \lambda_f = \lambda_a \lambda_c + \lambda_b \lambda_d$. Here the shear coordinates Z and $-Z$ of Fig. 2 (indicated by bold lines) are logarithms of the corresponding cross-ratios of λ -lengths (indicated by dashed lines) and we use the Poincaré disc model to represent the hyperbolic plane.

2.3. Flip morphisms of fat graphs. There are two sorts of flip morphisms (see Theorem 2.4 here below): morphisms induced by flips of inner edges and morphisms induced by flips of edges that are adjacent to a loop; we describe these two cases in the following two sub-sections. For convenience here below we drop the indices g, s_o, s_h as these numbers are preserved by the flip morphisms.

2.3.1. Flipping inner edges. Given a spine \mathcal{G} of Σ , if an internal edge α is neither a loop nor is adjacent to a loop, we may produce another spine \mathcal{G}_α of Σ by contracting and expanding edge α of \mathcal{G} , the edge labeled Z in Figure 2. We say that \mathcal{G}_α arises from \mathcal{G} by a *Whitehead move* (or flip) along the edge α . A labeling of edges of the spine \mathcal{G} implies a natural labeling of edges of the spine \mathcal{G}_α ; we then obtain a morphism between the spines \mathcal{G} and \mathcal{G}_α .

It was shown in [6] that setting $\phi(Z) = \log(1 + e^Z)$ and adopting the notation of Fig. 2 for shear coordinates of nearby edges, the effect of a flip is

$$\begin{aligned}
 W_Z : (A, B, C, D, Z) &\rightarrow (A + \phi(Z), B - \phi(-Z), C + \phi(Z), D - \phi(-Z), -Z) \\
 (2.11) \quad &:= (\tilde{A}, \tilde{B}, \tilde{C}, \tilde{D}, \tilde{Z}).
 \end{aligned}$$

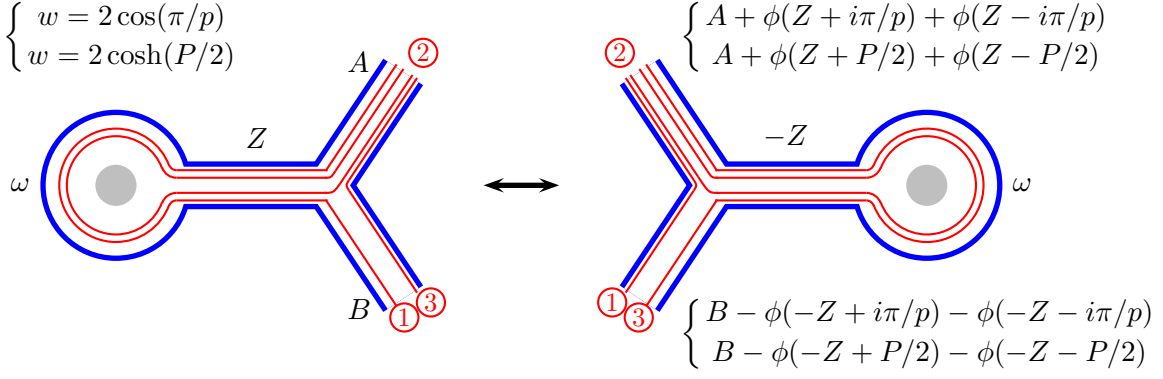


FIGURE 4. The transformation of dual variables (h -lengths) when flipping an edge incident to a loop; either $w = 2 \cos(\pi/p)$ or $w = 2 \cosh(P/2)$. We indicate how geodesic lines change upon flipping the edge.

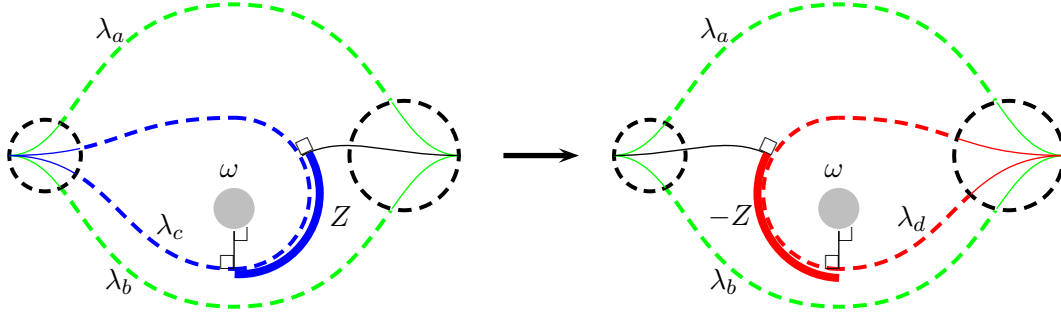


FIGURE 5. The transformation dual to the flip in Fig. 4: the flip, or mutation transformation, for the λ -lengths in this case is described by the generalised cluster relation $\lambda_c \lambda_d = \lambda_a^2 + \lambda_b^2 + \omega \lambda_a \lambda_b$. Here the shear coordinates Z and $-Z$ of Fig. 4 (indicated by bold lines) are logarithms of the corresponding cross-ratios of λ -lengths (indicated by dashed lines).

The same flip morphism for the dual λ -lengths is depicted in Fig. 3. The corresponding *mutation* is originated from the Ptolemy relation $\lambda_e \lambda_f = \lambda_a \lambda_c + \lambda_b \lambda_d$ [45] valid for every decorated ideal quadrangle.

The following lemma establishes the properties of invariance of geodesic functions w.r.t. the flip morphisms [7].

Lemma 2.2. *Transformation (2.11) preserves the traces of products over paths (2.9) (the geodesic functions) and transformation (2.11) simultaneously preserves Poisson structure (2.10) on the shear coordinates.*

Proof. The proof of this lemma is an elementary consequence of the following matrix equalities that can be established by simple calculations:

$$(2.12) \quad X_D R X_Z R X_A = X_{\tilde{A}} R X_{\tilde{D}},$$

$$(2.13) \quad X_D R X_Z L X_B = X_{\tilde{D}} L X_{\tilde{Z}} R X_{\tilde{B}},$$

$$(2.14) \quad X_C L X_D = X_{\tilde{C}} L X_{\tilde{Z}} L X_{\tilde{D}}.$$

Note that each of the above equalities corresponds to three geodesic cases in Fig. 2). \square

2.3.2. Flipping the edge incident to a loop.

Lemma 2.3. ([14],[10]) *The transformation in Fig. 4*

$$(2.15) \quad \begin{aligned} \{\tilde{A}, \tilde{B}, \tilde{Z}\} &:= \{A + \phi(Z + i\pi/p) + \phi(Z - i\pi/p), B - \phi(-Z + i\pi/p) - \phi(-Z - i\pi/p), -Z\}, \\ w &= 2 \cos(\pi/p); \end{aligned}$$

$$(2.16) \quad \begin{aligned} \{\tilde{A}, \tilde{B}, \tilde{Z}\} &:= \{A + \phi(Z + P/2) + \phi(Z - P/2), B - \phi(-Z + P/2) - \phi(-Z - P/2), -Z\}, \\ w &= 2 \cosh(P/2); \end{aligned}$$

where $\phi(x) = \log(1 + e^x)$, is a morphism of the space $\mathfrak{T}_{g,s_h,s_o}^H$ that preserves both Poisson structures (2.10) and the geodesic functions.

Proof. In this case, again, verifying the preservation of Poisson relations (2.10) is simple, while to show that traces over paths are preserved we need to consider three different cases, and in each of these cases we again obtain 2×2 -matrix equalities to be verified directly:

$$(2.17) \quad X_A L X_Z (F_\omega \Omega) X_Z L X_B = X_{\tilde{A}} R X_{\tilde{Z}} (-\Omega) X_{\tilde{Z}} R X_{\tilde{B}},$$

$$(2.18) \quad X_A L X_Z \Omega X_Z R X_A = X_{\tilde{A}} R X_{\tilde{Z}} (-\Omega) X_{\tilde{Z}} L X_{\tilde{A}},$$

$$(2.19) \quad X_B R X_Z \Omega X_Z L X_B = X_{\tilde{B}} L X_{\tilde{Z}} (-\Omega) X_{\tilde{Z}} R X_{\tilde{B}},$$

where Ω is any matrix commuting with F_ω ; explicitly $\Omega = \begin{pmatrix} a & c \\ -c & a - wc \end{pmatrix}$, $a, c \in \mathbb{C}$; in particular,

we can take F_ω^k , $k \in \mathbb{Z}$. □

The transformation (mutation) of dual λ -lengths is depicted in Fig. 5. It is described by the general cluster transformations of [14]: $\lambda_c \lambda_d = \lambda_a^2 + \lambda_b^2 + \omega \lambda_a \lambda_b$. The shear coordinate Z of the edge incident to a loop is the signed geodesic distance between perpendiculars to the third edge c of the ideal triangle abc through the vertex of this ideal triangle and between the hole (orbifold point) inside the monogon and the edge c (see Fig. 5). This signed distance is related to the cluster variables λ_a and λ_b by a simple formula (its proof is a nice exercise in hyperbolic geometry),

$$(2.20) \quad e^Z = \frac{\lambda_b}{\lambda_a}.$$

If, after a series of morphisms, we come to a graph of the same combinatorial type as the initial one (disregarding labeling of edges but distinguishing between different types of orbifold points and holes with different perimeters), we associate a *mapping class group* operation to this morphism therefore passing from the groupoid of morphisms to the group of modular transformations.

Remark 2.4. In the notation adopted in this paper, the only effect of changing the decoration (spiraling direction) of a hole inside a monogon corresponds to changing $P_i \rightarrow -P_i$ thus leaving invariant $w_i = 2 \cosh(P_i/2)$, so this transformation acts like the identity on the coordinates of $\mathfrak{T}_{g,s_h,s_o}^H$.

We can summarize as follows.

Theorem 2.4. *The whole mapping class group of Σ_{g,s_h,s_o} is generated by morphisms described by Lemmas 2.2 and 2.3.*

2.4. Quantum MCG transformations. We now quantize a Teichmüller space $\mathfrak{T}_{g,s_h,s_o}^H$ equivariantly w.r.t. the mapping class group action.

Let $\mathfrak{T}^h(\mathcal{G}_{g,s_h,s_o})$ be a $*$ -algebra generated by the generator Z_α^h (one generator per one unoriented edge α) and relations

$$(2.21) \quad [Z_\alpha^h, Z_\beta^h] = 2\pi i \hbar \{Z_\alpha, Z_\beta\}$$

with the $*$ -structure

$$(2.22) \quad (Z_\alpha^h)^* = Z_\alpha^h.$$

Here Z_α and $\{\cdot, \cdot\}$ stand for the respective coordinate functions on the classical Teichmüller space and the Weil–Petersson Poisson bracket on it. Note that according to formula (2.10), the right-hand side of (2.21) is merely a constant which may take only five values: $0, \pm 2\pi i\hbar, \pm 4\pi i\hbar$.

In the following two-subsection we quantize the flip morphisms viewed in sub-sections 2.3.1 and 2.3.2. We shall see that in each case the preservation of the commutation relations under quantum flip morphisms straightforward, while to verify the preservation of geodesic function operators requires some care.

Here and hereafter, for the rest of the paper, we assume that the ordering of quantum operators in a product is *natural*, i.e., it is determined by the order of matrix multiplication itself.

For the notation simplicity in what follows we omit the superscript \hbar for the quantum operators; the classical or quantum nature of the object will be always clear from the context.

2.4.1. *Quantum flip morphisms for inner edges.* It was proved in [6] that the *quantum flip morphisms*

$$(2.23) \quad \begin{aligned} \{A, B, C, D, Z\} &\rightarrow \{A + \phi^\hbar(Z), B - \phi^\hbar(-Z), C + \phi^\hbar(Z), D - \phi^\hbar(-Z), -Z\} \\ &:= \{\tilde{A}, \tilde{B}, \tilde{C}, \tilde{D}, \tilde{Z}\}, \end{aligned}$$

where A, B, C, D , and Z are as in Fig. 2 and $\phi^\hbar(x)$ is the real function of one real variable,

$$(2.24) \quad \phi^\hbar(z) = -\frac{\pi\hbar}{2} \int_{\Omega} \frac{e^{-ipz}}{\sinh(\pi p) \sinh(\pi\hbar p)} dp,$$

(the contour Ω goes along the real axis bypassing the singularity at the origin from above) satisfy the standard two-, four-, and five-term relations. The quantum dilogarithm function $\phi^\hbar(z)$ was introduced in this context by Faddeev in [18] and used in [17] for constructing quantum MCG transformations for the Liouville model, see, e.g., [6] for the properties of this function.

Remark 2.5. Note that exponentiated algebraic elements $U_i = e^{\pm Z_i}$, which obey homogeneous commutation relations $q^n U_i U_j = U_j U_i q^{-n}$ with $[X_i, X_j] = 2ni\pi\hbar$ and $q := e^{i\pi\hbar}$ transform as rational functions: for example, $e^{A+\phi^\hbar(Z)} = (1 + qe^Z)e^A$.

The quantum analogues of *matrix* relations (2.12)–(2.14) were found in [13]. Then, remarkably, *all four* entries of the corresponding 2×2 -matrices transform uniformly.

Lemma 2.5. [13] *Applying the quantum MCG transformation (2.23) to the curves 1, 2, and 3 in Fig. 2, we obtain the respective quantum matrix relations:*

$$(2.25) \quad X_D R X_Z R X_A = q^{1/4} X_{\tilde{D}} R X_{\tilde{A}},$$

$$(2.26) \quad X_D R X_Z L X_B = X_{\tilde{D}} R X_{\tilde{Z}} L X_{\tilde{B}},$$

$$(2.27) \quad X_D L X_C = q^{1/4} X_{\tilde{D}} L X_{\tilde{Z}} L X_{\tilde{C}}.$$

2.4.2. *Quantum flip morphisms for loops.*

Lemma 2.6. [10] *The transformation in Fig. 4*

$$(2.28) \quad \{\tilde{A}, \tilde{B}, \tilde{Z}\} := \{A + \phi^\hbar(Z + i\pi/p) + \phi^\hbar(Z - i\pi/p), B - \phi^\hbar(-Z + i\pi/p) - \phi^\hbar(-Z - i\pi/p), -Z\},$$

with $\phi^\hbar(x)$ from (2.24) and $w = 2\cos(\pi/p)$ or the transformations

$$(2.29) \quad \{\tilde{A}, \tilde{B}, \tilde{Z}\} := \{A + \phi^\hbar(Z + P/2) + \phi^\hbar(Z - P/2), B - \phi^\hbar(-Z + P/2) - \phi^\hbar(-Z - P/2), -Z\},$$

for $w = 2\cosh(P/2)$ are morphisms of the quantum $*$ -algebra $\mathfrak{T}_{g, s_h, s_o}^\hbar$.

The quantum versions of MCG transformations (2.17)–(2.19) are given here:

Lemma 2.7. [10] *We have the following quantum matrix relations:*

$$(2.30) \quad X_A L X_Z (F_p \Omega) X_Z L X_B = q^{-1} X_{\tilde{A}} R X_{\tilde{Z}} (-\Omega) X_{\tilde{Z}} R X_{\tilde{B}},$$

$$(2.31) \quad X_A L X_Z \Omega X_Z R X_A = X_{\tilde{A}} R X_{\tilde{Z}} (-\Omega) X_{\tilde{Z}} L X_{\tilde{A}},$$

$$(2.32) \quad X_B R X_Z \Omega X_Z L X_B = X_{\tilde{B}} L X_{\tilde{Z}} (-\Omega) X_{\tilde{Z}} R X_{\tilde{B}}.$$

Remark 2.6. Transformation laws (2.25)–(2.27) and (2.30)–(2.32) become identities without q -factors if we scale the matrices of right and left turns:

$$(2.33) \quad L \rightarrow q^{1/4} L, \quad R \rightarrow q^{-1/4} R.$$

Unfortunately, this property does not allow formulating a “working” ordering prescription for a general geodesic function. Indeed, we can use these transformations for bringing *any* simple closed loop geodesic function G_γ not homeomorphic to a hole to a form $G_\gamma = \text{tr } R X_{\tilde{Z}} L X_{\tilde{Y}}$ in some transformed shear coordinates \tilde{Z} and \tilde{Y} with the natural ordering assumed. But G_γ becomes a Hermitian operator in the Weyl ordered form, not in the naturally ordered one, so when passing to a naturally ordered expressions we must introduce different q -factors for different Laurent monomials in the expansion of G_γ , and these q -factors become uncontrollably spread over terms of the expansion of G_γ in the original shear coordinates.

Fortunately, for arcs, or λ -lengths in Sec. 5, powers of q factors coincide for *all* terms under the trace sign, which allows us to solve the problem of quantum ordering completely.

3. COLLIDING HOLES: NEW GEODESIC LAMINATIONS AND THE CORRESPONDING GEODESIC ALGEBRAS

In this section, we consider degenerations of stable Riemann surfaces that correspond to colliding two holes or two sides of the same hole of the original Riemann surface. Below we show that this results in the appearance of bordered Riemann surfaces with holes and with marked points on the boundaries of these holes represented by *bordered cusps*.

A Riemann surface $\Sigma_{g,s,n}$ of genus g with $s > 0$ holes/orbifold points and with $n \geq 0$ bordered cusps assigned to holes (no bordered cusps can be assigned to orbifold points) is called *stable* if its hyperbolic area (with tubular domains of holes removed) is positive. For a stable Riemann surface $\Sigma_{g,s,n}$ of genus g with $s_h > 0$ holes, s_o orbifold points of respective orders $2 \leq k_i < \infty$, $i = 1, \dots, s_o$ ($s := s_h + s_o$), and n bordered cusps, its hyperbolic area is (recall that every ideal triangle has area π)

$$\text{Area of } \Sigma_{g,s,n} = \left[4g - 4 + 2s_h + \sum_{i=1}^{s_o} \left(2 - \frac{2}{k_i} \right) + n \right] \pi = \left[4g - 4 + 2s + n - 2 \sum_{i=1}^{s_o} \frac{1}{k_i} \right] \pi.$$

So, all surfaces with $g > 0$ are stable (recall that we require $s_h > 0$ for any Riemann surface under consideration) and we have only a handful of nonstable cases at $g = 0$: ($s = 1; n = \{0, 1, 2\}$), ($s = 2; n = 0$), ($s_h = 1, s_o = 1$ ($k_1 = 2$); $n = 1$), ($s_h = 1, s_o = 2$ ($k_1 = k_2 = 2$); $n = 0$).

In our procedure of degenerations of stable Riemann surfaces, the total hyperbolic area will be preserved.

3.1. “Chewing gums” and degenerations of geodesic algebras. We are interested in the process of colliding two holes with geodesic boundaries on a Riemann surface. This means that we consider a limit in which the geodesic distance between these two holes tends to zero. In hyperbolic geometry, this means that we obtain a “thin” domain between these two holes, but the geodesic length of this domain, on the contrary, becomes infinite in this limit, see Fig. 6.^c

Instead of colliding two different holes, we can as well consider colliding two sides of the same hole.

^cIntuitively, it can be thought of as pulling a “chewing gum”: the hyperbolic area of the Riemann surface (with tubular domains of holes removed) is constant proportional to the Euler characteristics, so pulling a chewing gum we make it thinner in the middle.

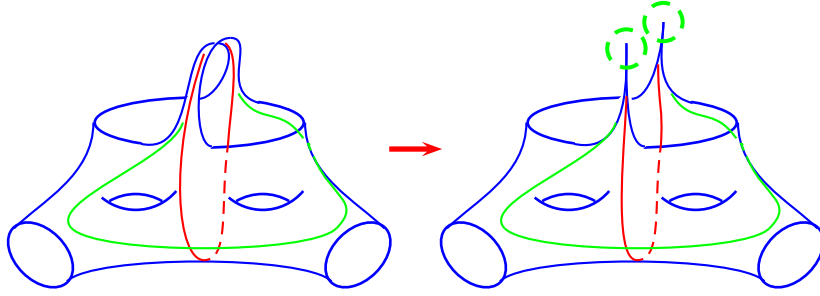


FIGURE 6. The process of colliding two holes on the Riemann surface $\Sigma_{g,s,0}$: as a result we obtain a Riemann surface $\Sigma_{g,s-1,2}$ of the same genus with one less hole, but with two new cusps on the boundary of this hole (indicated by a new index n : it increases by two in this process).

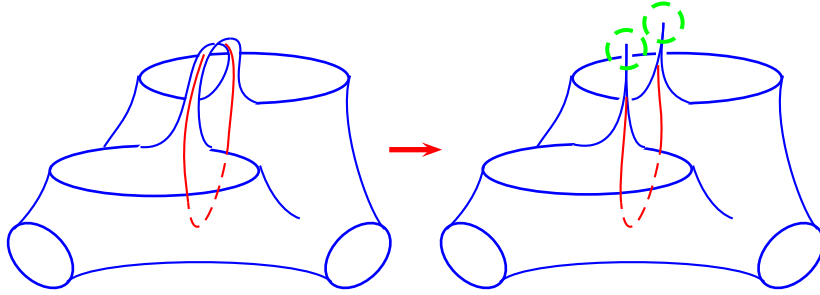


FIGURE 7. The process of colliding two sides of the same hole on the Riemann surface $\Sigma_{g,s,0}$ ($g > 0$): as a result we obtain a Riemann surface $\Sigma_{g-1,s+1,2}$ of genus lesser by one with one more hole and two new cusps on the boundaries of holes.

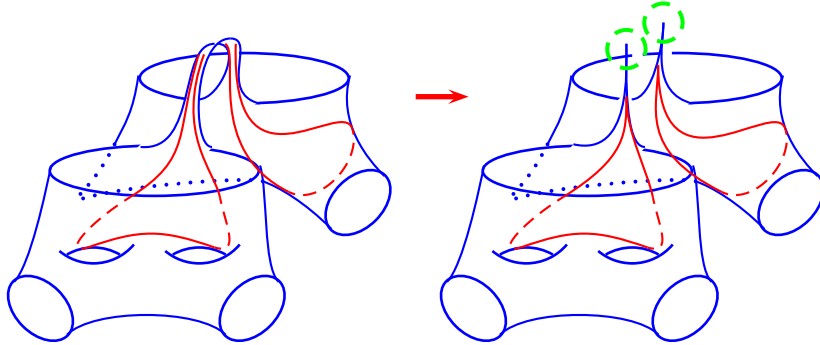


FIGURE 8. The process of colliding two sides of the same hole on the Riemann surface $\Sigma_{g,s,0}$ ($g > 0$) when it results in a two-component Riemann surfaces $\Sigma_{g_1,s_1,1}$ and $\Sigma_{g_2,s_2,1}$ with $g_1 + g_2 = g$ and $s_1 + s_2 = s + 1$: the hole splits into two holes on two different components, and each of the newly generated holes contains a new bordered cusp. A geodesic that passed through the corresponding “chewing gum” before breaking it (in this case, it must pass through it at least twice) splits into two geodesics starting and terminating at the newly created bordered cusps on two disjoint components.

We therefore have the following three types of processes:

1. The result of colliding two holes of a Riemann surface $\Sigma_{g,s,n}$ of genus g with s holes/orbifold points, and n bordered cusps is a Riemann surface of the same genus g , $s - 1$ holes/orbifold points, and $n + 2$ bordered cusps, and the hole obtained by colliding two original holes now contains two new bordered cusps (see Fig. 6).

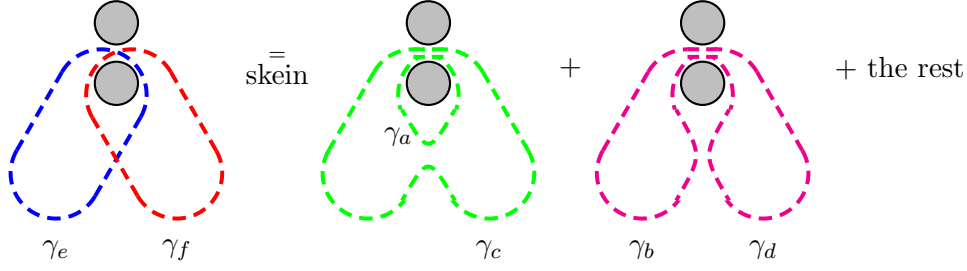


FIGURE 9. The skein relation applied to the geodesic functions of two geodesics (γ_e and γ_f) having a single intersection outside the “chewing gum” domain. As the result, we obtain the first term, which is a product of geodesic functions corresponding to geodesics γ_a and γ_c and the geodesic function that correspond to the geodesic that splits into two geodesics, γ_b and γ_d , when breaking the chewing gum. The rest is a combination of geodesic functions corresponding to geodesics not passing through the chewing gum domain.

2. The result of colliding sides of the same hole varies depending on whether breaking the chewing gum will result in one or two disjoint components (the latter happens unavoidably for example when the original surface has genus zero).

- 2a** If breaking the chewing gum constituted by sides of the same hole in $\Sigma_{g,s,n}$ results in a one-component surface, the new surface $\Sigma_{g-1,s+1,n+2}$ has genus lesser by one (so, originally, $g > 0$); the original hole then splits into two holes each containing one new bordered cusp (Fig. 7).
- 2b** If breaking the chewing gum constituted by sides of the same hole in $\Sigma_{g,s,n}$ results in a two-component surface, these new connected components, Σ_{g_1,s_1,n_1} and Σ_{g_2,s_2,n_2} , must be stable and such that $g_1 + g_2 = g$, $s_1 + s_2 = s + 1$, and $n_1 + n_2 = n + 2$ with $n_1 > 0$ and $n_2 > 0$ (Fig. 8).

As a result of these processes, new lamination patterns appear that incorporate both closed geodesics on the newly obtained Riemann surfaces with bordered cusps and *arcs*: geodesic paths starting and terminating at bordered cusps.

3.2. Limiting geodesic algebras. We now give a quantitative combinatorial description of geodesic laminations in the limit of breaking a chewing gum. For this, we present this process in the hyperbolic upper half-plane.

We begin with considering a useful example of a Riemann surface with at least two holes and two geodesics, γ_e and γ_f , passing between these two holes and having a single crossing in the rest of the Riemann surface. The corresponding skein relation reads

$$(3.1) \quad G_{\gamma_e} G_{\gamma_f} = G_{\gamma_a} G_{\gamma_c} + G_{\gamma_b \gamma_d} + \text{the rest},$$

where we let the rest denote combinations of geodesic functions for geodesics not passing through the chewing gum domain.

We now consider parts of geodesics “inside” a chewing gum (Fig. 10). We introduce the regularisation: two “collar lines” (dashed slanted straight lines in the figure): they are loci of points equidistant from the shortest geodesic joining boundaries of two holes (the vertical interval between 1 and $1 + \varepsilon$ on the y -axis). We now perform the limit as $\varepsilon \rightarrow 0$. In order to obtain finite answers for geodesic functions in this limit, we need to multiplicatively renormalise them:

$$(3.2) \quad G_\gamma \rightarrow G_\gamma e^{-D_\gamma/2},$$

where D_γ is the (total) geodesic length of the part(s) of the geodesic function passing through the chewing gum (if a geodesic does not pass through the chewing gum, it remains non-renormalized; if it passes more than once, then we take D_γ to be the total summed up lengths of all such parts).

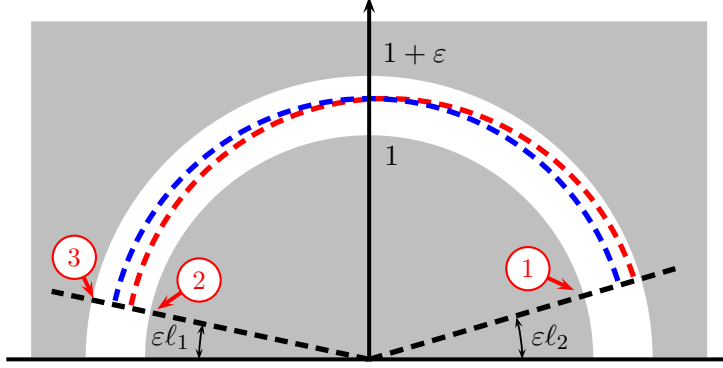


FIGURE 10. The part of the domain between colliding holes (painted grey). Collars that become boundaries of horocycles in the limit as $\varepsilon \rightarrow 0$ are slanted dashed straight lines; as $\varepsilon \rightarrow 0$ the distances between points 1 and 2 (D_{12}) and 1 and 3 (D_{13}) tend to infinity subject to the relation $e^{D_{12}/2} = (\varepsilon\sqrt{\ell_1\ell_2})^{-1} + O(\varepsilon)$, the width of the domain in the thinnest part (between the points $(0, 1)$ and $(0, 1 + \varepsilon)$) tends to zero whereas the length of the part of the collar between points 2 and 3 remains finite (tends to $1/\ell_1$ when $\varepsilon \rightarrow 0$). At the same time, all geodesic distances (parts of geodesic lines between the boundaries of two collars in the strip) are confined between D_{12} and D_{13} and the latter quantities satisfy the estimate $e^{D_{13}} = e^{D_{12}} + 1/(\ell_1\ell_2) + O(\varepsilon)$, so all differences between lengths of parts of geodesics confined in the part of the strip between two collars are of order $O(\varepsilon^2)$ as $\varepsilon \rightarrow 0$. We set $e^{\pi_i} := \ell_i$.

For simplicity consider the case where a geodesic passes once through the chewing gum. A remarkable fact is that although D_γ tends to infinity as $\varepsilon \rightarrow 0$, for any two geodesics γ_e and γ_f , the difference $D_{\gamma_e} - D_{\gamma_f}$ tends to zero. Indeed, for any such γ this distance satisfies the inequality $D_{12} < D_\gamma < D_{13}$ where D_{12} and D_{13} are geodesic distances between the corresponding points in Fig. 10. By using the formula relating hyperbolic distance $d_{\mathbb{H}}(z_1, z_2)$ between two points z_1, z_2 to the Euclidean one $|z_1 - z_2|$:

$$\left(\sinh \frac{d_{\mathbb{H}}(z_1, z_2)}{2} \right)^2 = \frac{|z_1 - z_2|^2}{4\operatorname{Im} z_1 \operatorname{Im} z_2},$$

we estimate

$$e^{D_{12}} \sim \frac{1}{\varepsilon^2 \ell_1 \ell_2} - \frac{(l_1 + l_2)^2}{4l_1 l_2} + \mathcal{O}(\varepsilon^2),$$

and

$$e^{D_{13}} \sim \frac{1}{\varepsilon^2 \ell_1 \ell_2} + \frac{4 - (l_1 + l_2)^2}{4l_1 l_2} + \mathcal{O}(\varepsilon),$$

so that:

$$e^{D_{13}} = e^{D_{12}} + \frac{1}{\ell_1 \ell_2} + O(\varepsilon),$$

and the difference $D_{12} - D_{13}$ is of order ε^2 at small ε .

We introduce the new variables π_i ,

$$(3.3) \quad e^{\pi_i} := \ell_i,$$

which become the new shear coordinates for decorated bordered cusps in the limit as $\varepsilon \rightarrow 0$. The distance D_{12} in terms of these variables reads

$$(3.4) \quad e^{D_{12}/2} = (\varepsilon)^{-1} e^{-\pi_1/2 - \pi_2/2}.$$

When we take the limit $\varepsilon \rightarrow 0$, the vertical interval between 1 and $1 + \varepsilon$ on the y -axis becomes a point infinitely distant from the rest of the Riemann surface, thus creating a cusp and a disconnected Riemann surface.

In the case where the result of breaking the chewing gum is a connected Riemann surface, as in Figs. 6 and 7, we can always choose a connected fundamental domain in \mathbb{H}_2^+ whose boundary contains two copies of the interval joining boundaries of holes. Indeed, if we first cut the surface along this interval

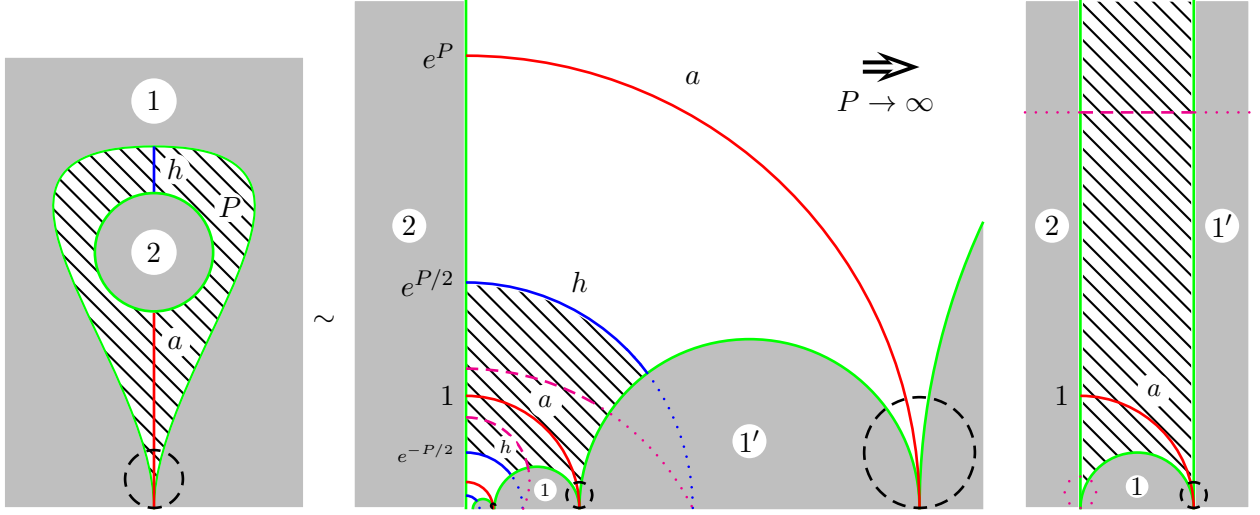


FIGURE 11. On the left we have the Riemann surface $\Sigma_{0,2,1}$: P is the perimeter of the inner hole, h is the shortest geodesic between the inner hole and the outer arc a ; h is related to P via the formula $\sinh^2(h/2) = (e^P - 1)^{-1}$ and tends to zero as $P \rightarrow \infty$. In the middle we depict the fundamental domain (hatched) obtained from the left picture by cutting along h , the only nontrivial hyperbolic element corresponding to rotation about the central hole acts by multiplication $z \rightarrow e^P z$, dashed lines are collars (which are segments of circles passing on the absolute (the real line) through the same points as half-circles corresponding to h). On the right we present the decorated ideal triangle (the Riemann surface $\Sigma_{0,1,3}$), which is the limit of the fundamental domain of $\Sigma_{0,2,1}$ as $P \rightarrow \infty$: in this limit, we obtain two new bordered cusps located at zero and infinity whereas collars transform into horocycles based at these bordered cusps.

we obtain these two copies whereas the remaining part is a connected surface which can be then cut along other lines until we obtain a simply connected (nonideal) polygon, which is a fundamental domain. Obviously, when cutting along the above interval breaks the Riemann surface in two disjoint parts (as in Fig. 8), in every such part we have only one copy of this interval and these two spaces become completely independent in the limit of breaking the chewing gum. A simplest example of this procedure for $\Sigma_{0,2,1}$ is depicted in Fig. 11.

We now consider the limit as $\varepsilon \rightarrow 0$ of skein relations (3.1) for two geodesics, γ_e and γ_f in Fig. 9. For this, we multiply this relation by $e^{-D_{12}} = \varepsilon^2 e^{\pi_1 + \pi_2}$ (because we have two geodesic lines passing through the chewing gum) and take the limit as $\varepsilon \rightarrow 0$. All terms corresponding to geodesics not passing through the chewing gum vanish and only the three terms in the figure contribute to the limiting relation. Chewing gum breaks into two *bordered cusps* whereas collar lines transform into *horocycles* decorating the corresponding cusps (see Fig. 12). Then, for the renormalised geodesic functions,

$$(3.5) \quad G_{\tilde{\gamma}} = \lim_{\varepsilon \rightarrow 0} G_{\gamma} e^{-D_{\gamma}/2} = \lim_{\varepsilon \rightarrow 0} \varepsilon G_{\gamma} e^{\pi_1/2 + \pi_2/2},$$

we obtain just the Ptolemy relation:

$$(3.6) \quad G_{\tilde{\gamma}_e} G_{\tilde{\gamma}_f} = G_{\tilde{\gamma}_a} G_{\tilde{\gamma}_c} + G_{\tilde{\gamma}_b} G_{\tilde{\gamma}_d},$$

in which the geodesic in the third term in (3.1) now splits into two new geodesics. Note that the thus obtained geodesic functions $G_{\tilde{\gamma}}$ are exponentials of halves of lengths of geodesics $\tilde{\gamma}$ confined between two horocycles (which can be the same horocycle):

$$(3.7) \quad \ell_{\tilde{\gamma}} = e^{D_{\tilde{\gamma}}/2}.$$

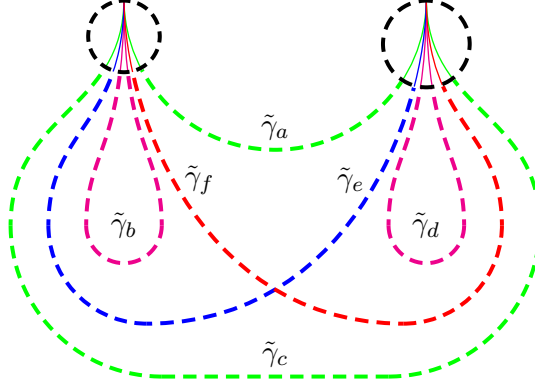


FIGURE 12. In the limit as $\varepsilon \rightarrow 0$ we obtain the Ptolemy relation for the new geodesic functions (corresponding to arcs).

That we have obtained the Ptolemy relation should not be surprising: indeed, since collars transform into horocycles in the above limit, the geodesics transform into λ -paths bounded by horocycles. What is more surprising is that we have an explicit way of doing this transition on the level of original shear coordinates.

The limit as $\varepsilon \rightarrow 0$ for shear coordinates of the original fat graph $\mathcal{G}_{g,s}$ corresponds to choosing the shear coordinate P_α of an edge whose sides are incident to two holes we are going to merge and replacing its exponential $e^{P_\alpha/2}$ by $1/\varepsilon$ simultaneously multiplying the whole expression by $\varepsilon e^{\pi_1/2+\pi_2/2}$. As the result, we obtain

$$(3.8) \quad X_{P_\alpha} \equiv \begin{bmatrix} 0 & -e^{P_\alpha/2} \\ e^{-P_\alpha/2} & 0 \end{bmatrix} \mapsto \begin{bmatrix} 0 & -1/\varepsilon \\ \varepsilon & 0 \end{bmatrix} \varepsilon e^{\pi_1/2+\pi_2/2} = \begin{bmatrix} 0 & -e^{\pi_1/2+\pi_2/2} \\ 0 & 0 \end{bmatrix} = X_{\pi_1} \begin{bmatrix} 0 & 0 \\ -1 & 0 \end{bmatrix} X_{\pi_2}.$$

So, we must merely replace X_{P_α} by $X_{\pi_1} K X_{\pi_2}$ where

$$(3.9) \quad K = \begin{pmatrix} 0 & 0 \\ -1 & 0 \end{pmatrix}$$

is the new matrix appearing because of reduction. Note that, for arbitrary 2×2 -matrices F_1, \dots, F_k ,

$$(3.10) \quad \text{tr}(F_1 K F_2 K \cdots F_n K) = \prod_{j=1}^n \text{tr}(F_j K),$$

so if an original geodesic was passing n times through the chewing gum, in the limit as $\varepsilon \rightarrow 0$ it will be partitioned into n disjoint geodesics each endowed with its own geodesic function $\text{tr}(F_i K)$.

4. COMBINATORIAL DESCRIPTION OF $\widehat{\mathfrak{T}}_{g,s,n}^H$

We now introduce the notion of Teichmüller space of Riemann surfaces with decorated bordered cusps in the case where we have at least one such cusp.

Definition 4.1. We denote by $\widehat{\mathfrak{T}}_{g,s,n}^H = \mathbb{R}^{6g-6+3s_{h_1}+2s_{h_o}+2n} \times \Omega^{s_{h_o}}$ the Teichmüller space of Riemann surfaces of genus g with $s_{h_1} > 0$ holes each of which contain at least one decorated bordered cusp, $s_{h_o} \geq 0$ holes/orbifold points not containing bordered cusps, and $n > 0$ decorated bordered cusps. An easy generalization of a similar statement in [14] claims that for any point $\{\pi_i, Z_\alpha, \omega_j\} \in \widehat{\mathfrak{T}}_{g,s,n}^H$ we have a metrizable Riemann surface $\Sigma_{g,s,n}$ with the prescribed distribution of decorated bordered cusps into boundary components and, vice versa, for any such Riemann surface $\Sigma_{g,s,n}$ we have a (nonunique) point in $\widehat{\mathfrak{T}}_{g,s,n}^H$ corresponding to this surface; in particular, the lengths of all geodesics and (decorated) arcs are then given in terms of generalized shear coordinates $\{\pi_i, Z_\alpha, \omega_j\} \in \widehat{\mathfrak{T}}_{g,s,n}^H$. We have a marking on the space of bordered cusps; every bordered cusp is associated to one of the holes, and we have

a natural cyclic ordering of bordered cusps associated to the same hole (this ordering is due to the orientation of the Riemann surface). MCG transformations can neither move a bordered cusp from one hole to another nor change the cyclic ordering of cusps associated to a given hole. Recall that every bordered cusp is decorated by a horocycle based at this cusp. The space $\widehat{\mathfrak{T}}_{g,s,n}^H$ is the space of the extended shear coordinates $\{\pi_i, Z_\alpha, \omega_j\}$ of a spine $\widehat{\mathcal{G}}_{g,s,n} \in \widehat{\Gamma}_{g,s,n}$ representing the corresponding Riemann surface and we let $\widehat{\Gamma}_{g,s,n}$ denote the set of all such spines.

Remark 4.2. Note that the above notion agrees with the real slice of the *decorated character variety* introduced in [12]. That construction is based on the fact that topologically speaking a Riemann surface $\Sigma_{g,s,n}$ with s holes, with n bordered cusps is equivalent to a Riemann surface $\tilde{\Sigma}_{g,s,n}$ of genus g , with s holes and n marked points m_1, \dots, m_n on the boundaries. Then the *fundamental groupoid of arcs* \mathfrak{U} is introduced as the set of all directed paths $\gamma_{ij} : [0, 1] \rightarrow \tilde{\Sigma}_{g,s,n}$ such that $\gamma_{ij}(0) = m_i$ and $\gamma_{ij}(1) = m_j$ modulo homotopy. The groupoid structure (a partial multiplication law) is induced by the standard path-composition rules.

Using the decoration by a horocycle at each cusp, one can associate to each arc γ_{ij} a matrix (denoted in the same way) $\gamma_{ij} \in SL_2(\mathbb{R})$ as explained in the previous section. The Teichmüller space $\widehat{\mathfrak{T}}_{g,s,n}^H$ is then defined as:

$$\text{Hom}(\mathfrak{U}, SL_2(\mathbb{R})) / \prod_{j=1}^n B_j,$$

where B_j is the Borel subgroup in $SL_2(\mathbb{R})$ (one Borel subgroup for each cusp).

4.1. Fat graph description for Riemann surfaces with holes, orbifold points, and decorated bordered cusps.

Definition 4.3. We call a fat graph (a graph with a prescribed cyclic ordering of edges entering each vertex) $\mathcal{G}_{g,s,n} \in \Gamma_{g,s,n}$ a *spine of the Riemann surface* $\Sigma_{g,s,n}$ with g handles, $s_{h_1} > 0$ holes containing bordered cusps, $s_{h_o} \geq 0$ holes/orbifold points not containing bordered cusps, and $n > 0$ decorated bordered cusps if

- (a) this graph can be embedded without self-intersections in $\Sigma_{g,s,n}$;
- (b) all vertices of $\mathcal{G}_{g,s,n}$ are three-valent except exactly n one-valent vertices (endpoints of the open edges), which are placed at the corresponding bordered cusps;
- (c) upon cutting along all *nonopen* edges of $\mathcal{G}_{g,s,n}$ the Riemann surface $\Sigma_{g,s,n}$ splits into s polygons each containing exactly one hole or orbifold point and being simply connected upon contracting this hole or erasing the orbifold point.
- (d) For a special subset $\widehat{\Gamma}_{g,s,n} \subset \Gamma_{g,s,n}$ of fat graphs, the above polygons are actually monogons for *all* orbifold points and *all* holes to which no bordered cusps are associated.

Therefore, for every spine $\widehat{\mathcal{G}}_{g,s,n} \in \widehat{\Gamma}_{g,s,n}$, every orbifold point and every hole with no associated bordered cusps is contained inside a closed loop, which is an edge starting and terminating at the same three-valent vertex. Vice versa, every such closed loop corresponds either to an orbifold point or to a hole with no associated bordered cusps. In what follows, we mainly consider these spines distinguishing them by the “hat” symbol.

Because every open edge corresponding to a bordered cusp “protrudes” towards the interior of some face of the graph, and we have exactly one hole contained inside this face, every fat graph $\mathcal{G}_{g,s,n} \in \Gamma_{g,s,n}$ determines a natural partition of the set of bordered cusps into nonintersecting (maybe empty) subsets δ_k , $k = 1, \dots, s_h$ of cusps incident to the corresponding holes, and in every such set we have the natural cyclic ordering coming from the orientation of the Riemann surface.

Edges of a graph $\widehat{\mathcal{G}}_{g,s,n}$ have the following labelling: to every edge that is neither open, nor a loop we set into the correspondence a real number Z_α ; to every open edge we set into correspondence a real number π_i , to every loop we set into the correspondence the number ω_j equal to $2 \cosh(P_j/2)$ for a hole with the perimeter $P_j \geq 0$ (the vanishing perimeter corresponds to a puncture) or equal to $2 \cos(\pi/r_j)$ for a \mathbb{Z}_{r_j} -orbifold point.

Remark 4.4. We can relax the condition (d) in Definition 4.3 for holes (not orbifold points) enlarging therefore the set of mapping class group transformations. This would be in line with [25, 24] where tagged cluster varieties were introduced. The aim to impose this restriction in this paper is twofold: first, it allows considering holes without cusps and orbifold points on an absolutely equal footing based on generalised cluster transformations of [14]. Second, in this case, we are able to establish an isomorphism between the sets of shear coordinates of $\widehat{\mathcal{G}} \in \widehat{\Gamma}_{g,s,n}$ and cluster variables in an explicit and simple way, which enables us to quantize the corresponding cluster variables in Sec. 5.

Definition 4.5. We call geometric *cusped geodesic lamination* (CGL) on a bordered cusped Riemann surface a set of nondirected curves up to a homotopic equivalence such that

- (a) these curves are either closed curves (γ) or *arcs* (\mathbf{a}) that start and terminate at bordered cusps (which can be the same cusp);
- (b) these curves have no (self)intersections inside the Riemann surface (but can be incident to the same bordered cusp);
- (c) these curves are not empty loops or empty loops starting and terminating at the same cusp.

Note that in each thus defined CGL sets of ends of arcs entering the same bordered cusp are *linearly ordered* w.r.t. the orientation of the Riemann surface.

We now set an algebraic cusped geodesic lamination into correspondence to its geometric counterpart.

Definition 4.6. The algebraic CGL corresponding to a geometric CGL is

$$(4.1) \quad \prod_{\gamma \in CGL} (2 \cosh(l_\gamma/2)) \prod_{\mathbf{a} \in CGL} e^{l_{\mathbf{a}}/2} := \prod_{\gamma \in CGL} G_\gamma \prod_{\mathbf{a} \in CGL} G_{\mathbf{a}}$$

where l_γ are the geodesic lengths of the corresponding closed curves and $l_{\mathbf{a}}$ are the signed geodesic lengths of the parts of arcs \mathbf{a} contained between two horocycles decorating the corresponding bordered cusps; the sign is negative when these horocycles intersect. The geodesic functions $G_\gamma = 2 \cosh(l_\gamma/2)$ for closed curves, as before, and $G_{\mathbf{a}} = e^{l_{\mathbf{a}}/2}$ for arcs.

Remark 4.7. The very important remark is that thus defined arcs are nothing but λ -lengths on the corresponding bordered cusped Riemann surfaces (see [25, 24]).

We next provide a quantitative description of the algebraic geodesic laminations. As in Sec. 2 we evaluate geodesic functions as traces of products of 2×2 -matrices by the following rules.

- We first choose the direction on a path or on an arc (the final result does not depend on this choice). We also choose the starting edge: for a closed path it can be any edge, for an arc we choose it to be a openedge of the “starting” bordered cusp.
- We take the product of 2×2 -matrices from right to left accordingly to the chosen direction: every time the path goes through an edge (labeled α) not incident to a loop we insert the *edge matrix* X_{Z_α} (2.4), where Z_α is the shear coordinate of the corresponding edge, which can be a open edge (starting or terminating); every time it makes a right or left turn at a three-valent vertex not incident to a loop we insert the corresponding matrices R and L (2.5); every time it goes along the edge (with the shear coordinate Z_β) incident to a loop, then along the loop with the parameter ω , then back along the same edge, we introduce the product of matrices $X_{Z_\beta} F_\omega X_{Z_\beta}$ if the path goes (once) clockwise along the loop or the product of matrices $X_{Z_\beta} (-F_\omega^{-1}) X_{Z_\beta}$ if it goes (once) counterclockwise F_ω is defined in (2.6); if a path goes makes more than one tour along the loop, it intersects itself and cannot enter a CGL.
- When a path corresponding to an arc terminates at a decorated bordered cusp we insert the matrix K (3.9). We obtain the geodesic functions G_γ and $G_{\mathbf{a}}$ by taking the traces of the thus constructed products of matrices.

We now describe the geometric meaning of the new shear coordinates π_i associated with decorated bordered cusps. In the ideal triangle decomposition dual to a fat graph $\widehat{\mathcal{G}}_{g,s,n} \in \widehat{\Gamma}_{g,s,n}$, we establish a

1-1 correspondence between arcs and all edges of the graph that are not loops. For inner edges and edges adjacent to loops, the correspondence is as in Sec. 2, and we set into correspondence to an open edge terminating at a decorated bordered cusp the edge of the ideal triangle that is bordering the surface to the left (if looking from inside the surface) from this bordered cusp. We therefore allow arcs between neighbouring cusps to be included into laminations; these arcs actually play important role in our construction.

Explicitly, π_i is the geodesic distance between the perpendicular to the “outer” side of the triangle through the vertex opposite to this side and horocycle decorating the i th cusp (see Fig. 13). The relation to λ -lengths of edges of this triangle is

$$(4.2) \quad e^{\pi_i} = \frac{\lambda_c \lambda_b}{\lambda_a},$$

where the edges a , b , and c are as in the figure. The new shear coordinates are therefore hybrids of genuine shear coordinates and λ -lengths being distances between perpendiculars and horocycles.

Definition 4.8. We call a *maximum arc CGL*, denoted by CGL_a^{\max} , of a bordered cusped Riemann surface $\Sigma_{g,s,n}$ with $s > 0$ and $n > 0$ the collection of all edges of the following ideal-triangle decomposition of $\Sigma_{g,s,n}$: (a) all edges of ideal triangles terminate at bordered cusps; (b) all holes/orbifold points that do not contain bordered cusps are contained in monogons; (c) the rest of the surface obtained by eliminating all monogons containing holes/orbifold points without bordered cusps is partitioned into ideal triangles (all three sides of every such triangle are necessarily distinct).

Definition 4.9. Given a fat graph $\widehat{\mathcal{G}}_{g,s,n} \in \widehat{\Gamma}_{g,s,n}$ with $n > 0$ we have a unique CGL_a^{\max} dual to $\widehat{\mathcal{G}}_{g,s,n}$. This duality means that we can embed $\widehat{\mathcal{G}}_{g,s,n}$ into a Riemann surface $\Sigma_{g,s,n}$ partitioned into ideal triangles and monogons (containing holes/orbifold points without bordered cusps) by elements of CGL_a^{\max} in such a way that every internal edge of $\widehat{\mathcal{G}}_{g,s,n}$ that is not a loop intersects with exactly one (internal) arc from CGL_a^{\max} , every outer edge of $\widehat{\mathcal{G}}_{g,s,n}$ terminates at its own bordered cusp (and we set the bordered arc to the left of this cusp in correspondence to this edge), and every loop is homeomorphic to its ω -cycle from this lamination.

Vice versa, we obtain the fat graph $\widehat{\mathcal{G}}_{g,s,n} \in \widehat{\Gamma}_{g,s,n}$ (with $s > 0$ and $n > 0$) dual to a maximum arc CGL_a^{\max} as follows: we set three-valent vertices into correspondence to every monogon with a hole/orbifold point and to every ideal triangle placing these vertices inside the corresponding monogons (but outside holes contained inside monogons) and triangles. We then draw loops (edges starting and terminating at the same vertex) around holes/orbifold points inside monogons; all other internal edges of $\widehat{\mathcal{G}}_{g,s,n}$ joint pairwise distinct neighbor three-valent vertices; each edge crosses exactly one arc from CGL_a^{\max} and we have exactly n “outer” edges starting at three-valent vertices of $\widehat{\mathcal{G}}_{g,s,n}$ and terminating at the bordered cusps; these edges correspond to n bordering arcs (framing holes with bordered cusps), and for each such arc the corresponding edge terminates at the “right” bordered cusp incident to this arc (when looking from inside the Riemann surface). All edges of this fat graph are endowed with real numbers (shear coordinates): edges that are neither loops nor “outer” edges (terminating at bordered cusps) are endowed with $Z_\alpha \in \mathbb{R}$, “outer” edges are endowed with $\pi_j \in \mathbb{R}$, and loops are endowed with $\omega_i = 2 \cosh(P_i/2)$, $P_i \in \mathbb{R}$, for holes and $\omega_i = 2 \cos(\pi/p_i)$, $p_i \in \mathbb{Z}_{\geq 2}$, for orbifold points.

For the dual graph, we have the following inversion formula expressing λ -lengths of arcs from CGL_a^{\max} in terms of the extended shear coordinates of the dual fat graph.

Proposition 4.1. *Given a CGL_a^{\max} and its dual fat graph $\widehat{\mathcal{G}}_{g,s,n}$, every arc $\alpha_\alpha \in \text{CGL}_a^{\max}$ intersects exactly one edge of $\widehat{\mathcal{G}}_{g,s,n}$ labeled α and carrying the shear coordinate Z_α ; the λ -length of this arc reads*

$$\begin{aligned} \lambda_\alpha &= \text{tr} \left[K X_{\pi_2^{(\alpha)}} R X_{Y_1} R X_{Y_2} R \cdots R X_{Y_i} F_{\omega_i} X_{Y_i} R \cdots R X_{Y_s} R X_{Z_\alpha} L X_{Z_1} L \cdots L X_{Z_r} F_{\omega_r} X_{Z_r} L \cdots L X_{Z_k} L X_{\pi_1^{(\alpha)}} \right] \\ &= \exp \left[(\pi_1^{(\alpha)} + \pi_2^{(\alpha)} + Y_1 + Y_2 + \cdots + 2Y_i + \cdots + Y_s + Z_\alpha + Z_1 + \cdots + 2Z_r + \cdots + Z_k)/2 \right] \end{aligned}$$

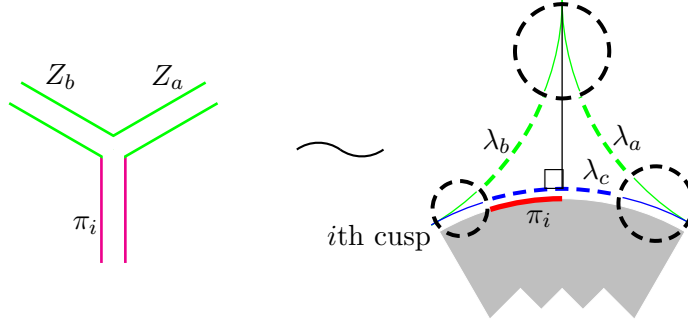


FIGURE 13. The shear coordinate of an open edge corresponding to the i th decorated bordered cusp. On the left-hand side we present a part of a fat graph with the open edge endowed with the variable π_i ; on the right-hand side we present the corresponding ideal triangle whose side corresponding to π_i borders a hole (other sides can also border holes or can be adjacent to loops), the shear coordinate of this edge is $e^{\pi_i} = (\lambda_c \lambda_b / \lambda_a)$ and it is sensitive only to the decoration at the i th bordered cusp.

if this edge is not incident to a loop; if it is incident to a loop, then

$$\begin{aligned} \lambda_\alpha &= \text{tr} \left[K X_{\pi_1^{(\alpha)}} R X_{Z_1} R X_{Z_2} R \cdots R X_{Z_{\alpha-1}} R X_{Z_\alpha} F_{\omega_\alpha} X_{Z_\alpha} L X_{Z_{\alpha-1}} L \cdots L X_{Z_1} L X_{\pi_1^{(\alpha)}} \right] \\ &= \exp \left[\pi_1^{(\alpha)} + Z_1 + \cdots + Z_\alpha \right], \end{aligned}$$

so in both cases, the corresponding λ -lengths are monomial products of $e^{+Z_s/2}$ where the index s ranges all edges (with multiplicities) passed by the corresponding arc. The inverse transformations expressing $\{Z_\alpha, \pi_j\}$ through λ_a are (2.3), (2.20), and (4.2).

Remark 4.10. Our construction is obviously non symmetric w.r.t. changing the orientation of the surface. Instead of taking the limit as $P_\alpha \rightarrow +\infty$ in (3.8) we may take the limit as $P_\alpha \rightarrow -\infty$ in the same expression. This will then result in the insertion of the matrix $K' = \begin{pmatrix} 0 & 1 \\ 0 & 0 \end{pmatrix}$ instead of the matrix (3.9) in the proper places, and the shear variable π_i will then be based on the ideal triangle that is to the right, not to the left, from the corresponding bordered cusp. Nevertheless, components of geodesic laminations remain to be $G_a = e^{+l_a/2}$ with the same definition of the signed length (with the plus sign for nonintersecting horocycles).

4.2. Morphisms of shear coordinates on $\widehat{\mathfrak{T}}_{g,s,n}^H$. In the case where we consider the set of fat graphs $\widehat{\Gamma}_{g,s,n}$ with $n > 0$ all morphisms of shear coordinates on $\widehat{\mathfrak{T}}_{g,s,n}^H$ are generated by flips (mutations) of inner edges (not adjacent to loops and not open) described by formula (2.11), by flips (mutations) of edges adjacent to loops described by Lemma 2.3, and neither loop edges nor open edges are allowed to mutate. This set of morphisms obviously acts inside the set $\widehat{\Gamma}_{g,s,n}$ provided we have at least one bordered cusp.

Remark 4.11. Restricting the set of admissible spines to that of $\widehat{\Gamma}_{g,s,n}$ we (intentionally) impose restrictions on the set of morphisms; one reason is that in this presentation we want to avoid further complications (and inflating the text volume) related to introducing *notching* of edges (see [25], [24]). thus postponing developing corresponding cluster structures to subsequent publications. Another important reason is that only for $\widehat{\mathcal{G}}_{g,s,n} \in \widehat{\Gamma}_{g,s,n}$ all dual cluster variables correspond to arcs between decorated bordered cusps (*regular arcs* in terminology of [24]). Although the extended shear coordinates $\{\pi_i, Z_\alpha\}$ are well defined for any $\widehat{\mathcal{G}}_{g,s,n} \in \widehat{\Gamma}_{g,s,n}$ and admit the Poisson algebras and quantization, only λ -lengths of ordinary arcs, not those of tagged arcs, can be expressed in terms of these extended

shear coordinates (for any spine from $\widehat{\Gamma}_{g,s,n}$) enabling us to derive Poisson and quantum algebras for these λ -lengths.

On the other hand, notching the edges terminating at holes without bordered cusps corresponds (see [25], [24]) to enlarging the lamination sets including geodesic lines winding to the geodesic boundaries of the corresponding holes (the notching then corresponds to choosing the winding direction). But because we obtain our system of lambda-lengths from colliding holes of an original Riemann surface endowed with a set of closed geodesic lines (which degenerate into arcs in the bordered cusped Riemann surfaces), we do not have geodesic lines winding to holes in the original formulation and we do not expect their appearance in the final expressions.

4.3. The skein relation for CGLs. In this section we introduce the skein relation for elements of new CGLs. Let us recall that the standard skein relation between two closed curves corresponds to the following trace relation valid for any two matrices in SL_2 :

$$\text{tr } A \text{tr } B = \text{tr } (AB) + \text{tr } (AB^{-1}).$$

We can still use this formula when the matrix A is no longer invertible, namely we can trivially extend the skein relation to the case of an arc and a closed curve. This means that by choosing $G_1 = \text{tr } A$ and $G_2 = \text{tr } B$ where B corresponds to a closed curve, we obtain that we can resolve their intersection in the standard way depicted in Fig. 14.

However, when both geodesic functions correspond to arcs, the above formula is no longer valid and we must use a more “refined” version which will turn out to be useful also when we want to quantise. To this aim, we first approach the skein relation from a purely algebraic view point. Let us consider the permutation matrix

$$P_{12} := \sum_{i,j} e_{i,j}^1 \otimes e_{j,i}^2,$$

where we use the standard notation for the matrix $e_{i,j}$ that has a unity at the intersection of i th row and j th column with all other elements equal to zero. It is not difficult to prove that for any two matrices A and B

$$\text{tr } (AB) = \text{tr}_{12} \left(\begin{smallmatrix} 1 & 2 \\ A & P_{12} B \end{smallmatrix} \right).$$

Let us now consider the transposition of the permutation matrix in one of the matrix spaces (does not matter in which as the total transposition leaves P_{12} invariant):

$$P_{12}^{T_1} = \sum_{i,j} e_{i,j}^1 \otimes e_{i,j}^2,$$

and introduce

$$\tilde{P}_{12} := \left(\begin{smallmatrix} 1 & 2 \\ F & \mathbb{I} \end{smallmatrix} \right) P_{12}^{T_1} \left(\begin{smallmatrix} 1 & 2 \\ F & \mathbb{I} \end{smallmatrix} \right),$$

where

$$F = \begin{pmatrix} 0 & 1 \\ -1 & 0 \end{pmatrix}.$$

Again it is not difficult to prove that for any matrix A and any matrix $B \in SL_2$, thanks to the fact that $B^{-1} = -FB^T F$, one has:

$$\text{tr } (AB^{-1}) = -\text{tr}_{12} \left(\begin{smallmatrix} 1 & 2 \\ A & \tilde{P}_{12} B \end{smallmatrix} \right),$$

so that the skein relation can be written as follows:

$$(4.3) \quad \text{tr } A \text{tr } B = \text{tr}_{12} \left(\begin{smallmatrix} 1 & 2 \\ A & P_{12} B \end{smallmatrix} \right) - \text{tr}_{12} \left(\begin{smallmatrix} 1 & 2 \\ A & \tilde{P}_{12} B \end{smallmatrix} \right)$$

It is easy to prove that this new version (4.3) of the skein relation is valid for any 2×2 matrices, non necessarily in SL_2 . Indeed it is a simple consequence of the fact that

$$(4.4) \quad \text{tr}(A)\text{tr}(B) = \text{tr}_{12} \begin{pmatrix} 1 & 2 \\ A & B \end{pmatrix} = \text{tr}_{12} \begin{pmatrix} 1 & 1 \\ A\mathbb{I} & \mathbb{I}B \end{pmatrix}$$

and

$$\begin{pmatrix} 1 & 2 \\ \mathbb{I} & \mathbb{I} \end{pmatrix} = P_{12} - \tilde{P}_{12}.$$

Now we match this algebraic explanation to the geometric picture. Since the matrices A and B describe arcs or geodesics, they will generically be given by some product of left, right, edge matrices and possibly a cusp matrix K as explained in sub-section 4.1. In particular for the skein relation to make sense geometrically, A and B must intersect, or in other words they must contain at least one edge matrix with the same coordinate, and the two right hand side terms in (4.3) must also define arcs or geodesics. For example, assume:

$$A = K \cdots L X_Z R \cdots \quad \text{and} \quad B = \cdots K \cdots R X_Z L \cdots$$

then the traces

$$(4.5) \quad \begin{aligned} \text{tr}(A) &= \text{tr} \left(\begin{pmatrix} 1 \\ K \end{pmatrix} \cdots \begin{pmatrix} 1 & 1 \\ L X_Z R \end{pmatrix} \begin{pmatrix} 1 \\ \cdots \end{pmatrix} \right) \\ \text{tr}(B) &= \text{tr} \left(\cdots \begin{pmatrix} 2 \\ K \end{pmatrix} \cdots \begin{pmatrix} 2 & 2 \\ R X_Z L \end{pmatrix} \begin{pmatrix} 2 \\ \cdots \end{pmatrix} \right), \end{aligned}$$

are invariant with respect to cyclic permutation. When using the relation (4.4), we must cyclically permute the building blocks in A and B as follows:

$$(4.6) \quad \begin{aligned} \text{tr}(A) &= \text{tr} \left(\begin{pmatrix} 1 \\ R \end{pmatrix} \cdots \begin{pmatrix} 1 \\ K \end{pmatrix} \cdots \begin{pmatrix} 1 & 1 \\ L X_Z \end{pmatrix} \right) \\ \text{tr}(B) &= \text{tr} \left(\begin{pmatrix} 2 \\ L \end{pmatrix} \cdots \begin{pmatrix} 2 \\ K \end{pmatrix} \cdots \begin{pmatrix} 2 & 2 \\ R X_Z \end{pmatrix} \right), \end{aligned}$$

so that now the two right hand side terms in (4.3) become:

$$\text{tr}_{12} \left(\begin{pmatrix} 1 \\ R \end{pmatrix} \cdots \begin{pmatrix} 1 \\ K \end{pmatrix} \cdots \begin{pmatrix} 1 & 1 \\ L X_Z \end{pmatrix} P_{12} \begin{pmatrix} 2 \\ L \end{pmatrix} \cdots \begin{pmatrix} 2 \\ K \end{pmatrix} \cdots \begin{pmatrix} 2 & 2 \\ R X_Z \end{pmatrix} \right) - \text{tr}_{12} \left(\begin{pmatrix} 1 \\ R \end{pmatrix} \cdots \begin{pmatrix} 1 \\ K \end{pmatrix} \cdots \begin{pmatrix} 1 & 1 \\ L X_Z \end{pmatrix} \tilde{P}_{12} \begin{pmatrix} 2 \\ L \end{pmatrix} \cdots \begin{pmatrix} 2 \\ K \end{pmatrix} \cdots \begin{pmatrix} 2 & 2 \\ R X_Z \end{pmatrix} \right).$$

To convince oneself that both these terms describe arcs we need to use the following two properties of P_{12} and \tilde{P}_{12} : for any matrix S :

$$P_{12} \begin{pmatrix} 1 \\ S \end{pmatrix} = \begin{pmatrix} 2 \\ S \end{pmatrix} P_{12}$$

and

$$\tilde{P}_{12} \begin{pmatrix} 2 \\ S \end{pmatrix} = \begin{pmatrix} 1 & 1 \\ F S \end{pmatrix} \begin{pmatrix} 1 \\ F \end{pmatrix} \tilde{P}_{12},$$

so that

$$\text{tr}_{12} \left(\begin{pmatrix} 1 \\ R \end{pmatrix} \cdots \begin{pmatrix} 1 \\ K \end{pmatrix} \cdots \begin{pmatrix} 1 & 1 \\ L X_Z \end{pmatrix} P_{12} \begin{pmatrix} 2 \\ L \end{pmatrix} \cdots \begin{pmatrix} 2 \\ K \end{pmatrix} \cdots \begin{pmatrix} 2 & 2 \\ R X_Z \end{pmatrix} \right) = \text{tr}_{12} \left(\begin{pmatrix} 1 \\ R \end{pmatrix} \cdots \begin{pmatrix} 1 \\ K \end{pmatrix} \cdots \begin{pmatrix} 1 & 1 \\ L X_Z \end{pmatrix} \begin{pmatrix} 1 & 1 \\ L \end{pmatrix} \cdots \begin{pmatrix} 1 \\ K \end{pmatrix} \cdots \begin{pmatrix} 1 & 1 \\ R X_Z \end{pmatrix} P_{12} \right),$$

which defines an arc by construction. Analogously:

$$\text{tr}_{12} \left(\begin{pmatrix} 1 \\ R \end{pmatrix} \cdots \begin{pmatrix} 1 \\ K \end{pmatrix} \cdots \begin{pmatrix} 1 & 1 \\ L X_Z \end{pmatrix} \tilde{P}_{12} \begin{pmatrix} 2 \\ L \end{pmatrix} \cdots \begin{pmatrix} 2 \\ K \end{pmatrix} \cdots \begin{pmatrix} 2 & 2 \\ R X_Z \end{pmatrix} \right) = \text{tr}_{12} \left(\begin{pmatrix} 1 \\ R \end{pmatrix} \cdots \begin{pmatrix} 1 \\ K \end{pmatrix} \cdots \begin{pmatrix} 1 & 1 \\ L X_Z \end{pmatrix} \begin{pmatrix} 1 & 1 \\ F X_Z \end{pmatrix} \begin{pmatrix} 1 \\ F \end{pmatrix} \cdots \begin{pmatrix} 1 \\ K \end{pmatrix} \cdots \begin{pmatrix} 1 & 1 \\ R F \end{pmatrix} \tilde{P}_{12} \right),$$

that, thanks to the fact that $X_Z^2 = F^2 = -\mathbb{I}$ and $FK^TF = K$, again defines an arc.

Let us now (4.3) implies the Ptolemy relation when both A and B correspond to arcs. Let us again proceed first by a purely algebraic point of view. Thanks to the results of section 4, we have:

$$A = A_1 K A_2, \quad B = B_1 K B_2,$$

where A_1, A_2, B_1, B_2 will be given by some products of left, right and edge matrices, or in other words they are elements of $SL_2(\mathbb{R})$ while K is defined in (3.9) and satisfies $FK^TF = K$. We then have

$$\text{tr}_{12} \left(\begin{pmatrix} 1 \\ A \end{pmatrix} P_{12} \begin{pmatrix} 2 \\ B \end{pmatrix} \right) = \text{tr}(A_1 K A_2 B_1 K B_2) = \text{tr}(B_2 A_1 K A_2 B_1 K) = \text{tr}(B_2 A_1 K) \text{tr}(A_2 B_1 K),$$

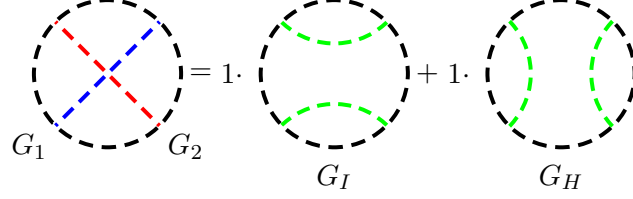


FIGURE 14. The classical skein relation: for an inner-point crossing of two curves γ_1 and γ_2 , the corresponding geodesic functions satisfy (4.8) where in the left-hand side we have two CGLs (comprising one curve each if at least one of γ_i is a closed curve and two arcs each if the both γ_i are arcs) obtained by two possible resolutions of the crossing.

due to the nice property of K that $\text{tr}(SKTK) = \text{tr}(SK)\text{tr}(TK)$ for any two matrices S and T . Analogously:

$$\begin{aligned} -\text{tr}_{12} \begin{pmatrix} 1 & \\ A & \tilde{P}_{12} & B \\ & & 2 \end{pmatrix} &= \text{tr}(AFB^T F) = \text{tr}(A_1 K A_2 F B_2^T K^T B_1^T F) = \text{tr}(A_1 K A_2 F B_2^T F^2 K^T F^2 B_1^T F) = \\ &= \text{tr}(A_1 K A_2 B_2^{-1} K B_1^{-1}) = \text{tr}(B_1^{-1} A_1 K) \text{tr}(A_2 B_2^{-1} K), \end{aligned}$$

so that in the end we obtain the Ptolemy relation:

$$(4.7) \quad \text{tr}(A_1 K A_2) \text{tr}(B_1 K B_2) = \text{tr}(B_2 A_1 K) \text{tr}(A_2 B_1 K) + \text{tr}(B_1^{-1} A_1 K) \text{tr}(A_2 B_2^{-1} K).$$

Here again to match this algebraic explanation to the geometric picture we assume that A and B contain at least one edge matrix with the same coordinate and we need to cyclically permute the building blocks in A and B in such a way that all terms on the right hand side of (4.7) define arcs. We leave this to the reader as it is analogous to the previous case.

So, in all cases we can still present the skein relations as in Fig. 14: for two curves γ_1 and γ_2 having a single crossing inside the Riemann surface, the corresponding geodesic functions $G_1 = \text{tr}(A)$ and $G_2 = \text{tr}(B)$ satisfy the relation

$$(4.8) \quad G_1 G_2 = G_I + G_H,$$

where any of G_1 and G_2 can be either closed curves or arcs, and we obtain the geodesic or arcs G_I and G_H by resolving the crossing locally in two ways shown in the figure. In the case of multiple crossings, we resolve them one at the time and it is straightforward to prove that the order in which we resolve the crossings does not change the final result.

We can then extend the skein relation to laminations: the skein relation between two CGLs, call them CGL_1 and CGL_2 reads

$$(4.9) \quad \text{CGL}_1 \text{CGL}_2 = \sum_{\text{resolutions}} \text{CGL}_{HIIHHI...},$$

where in the left-hand side we have the sum of CGLs obtained by applying resolutions to all crossings of CGL_1 and CGL_2 (for m crossings the left-hand side contains 2^m terms). If, in the resolution process, we obtain a closed empty loop, we assign the factor -2 to this loop (so not all terms come with plus sign in the left-hand side of (4.9)). If, in the resolution process, we obtain an empty loop starting and terminating at a bordered cusp, we assign zero to this curve thus killing the whole corresponding $\text{CGL}_{HIIHHI...}$. If a loop homeomorphic to going around hole/orbifold point appears, we substitute its parameter ω_i .

4.4. Open/closed string diagrammatics as a projective limit of λ -lengths. We now establish a correspondence between our description of Riemann surfaces with bordered cusps and the approach of *windowed surfaces* by Kaufmann and Penner [34]. The authors of [34] proposed to consider laminations on Riemann surfaces with marked points on boundary components determining *windows*: the domains between neighboring marked points; elements of laminations are allowed to escape through these

windows. In our approach, we naturally identify these windows with parts of horocycles confined between two bordered arcs. We then have the following *correspondence principle*:

Given a Riemann surface $\Sigma_{g,s,n}$ with $n > 0$, a fat graph $\widehat{\mathcal{G}}_{g,s,n} \in \widehat{\Gamma}_{g,s,n}$, and a lamination, which is a finite set of nonintersecting curves that are either closed or start and terminate at windows (see, e.g., Fig. 12 for examples of such curves), we can always collapse this lamination to $\widehat{\mathcal{G}}_{g,s,n}$ in such a way that all lines of the lamination terminating at a window will terminate at the corresponding bordered cusp. Then the parameters $\ell_\alpha \in \mathbb{Z}_{(+,0)}$ indicating how many lines of the lamination pass through the given (α th) edge are determined uniquely. We identify these parameters with the *projective limit* of λ -lengths of arcs: specifically, ℓ_α is the projective limit of $\log \lambda_\alpha$ where λ_α is the λ -length of the arc that is dual to the α th edge and belongs to a unique CGL_a^{\max} dual to $\widehat{\mathcal{G}}_{g,s,n}$.

The above identification is based on the fact that the *tropical limit* (or the projective limit) of mutations describes transformations of the variables ℓ_α upon flips; indeed, when flipping an inner edge as in Fig. 2, we obtain

$$(4.10) \quad \ell_e + \ell_f = \max[\ell_a + \ell_c, \ell_b + \ell_d],$$

and when flipping an edge incident to a loop as in Fig. 4 we have

$$(4.11) \quad \ell_e + \ell_f = \max[2\ell_a, 2\ell_b].$$

Here ℓ_e and ℓ_f are parameters of lamination for the original and transformed edges and in the right-hand sides of (4.10) and (4.11) we can easily recognize projective limits of the corresponding mutation formulas

$$(4.12) \quad [45] \quad \lambda_e \lambda_f = \lambda_a \lambda_c + \lambda_b \lambda_d,$$

$$(4.13) \quad [14] \quad \lambda_e \lambda_f = \lambda_a^2 + \omega \lambda_a \lambda_b + \lambda_b^2$$

obtained by taking the scaling limit $\lambda_\alpha \rightarrow e^{N\ell_\alpha/2}$ with the same $N \rightarrow +\infty$ for all α .

We therefore identify windows by Kaufmann and Penner with asymptotic domains (a decoration becomes irrelevant in the projective limit), which correspond in the open/closed string terminology to incoming/outgoing *open strings*; we thus have a convenient parameterization of an open/closed string worldsheet in terms of the extended shear coordinates provided we have at least one open string asymptotic state. The open/closed string worldsheet corresponding to $\Sigma_{g,s,n}$ then has genus g , has exactly n open string asymptotic states, and exactly s_{h_o} closed string asymptotic states (in the absence of conical singularities corresponding to orbifold points).

4.5. Comparing to the theory of bordered surfaces by Fomin, M. Shapiro, and D. Thurston.

In two nice papers by Fomin, M. Shapiro, and D. Thurston [25] and by Fomin and D. Thurston [24], the authors developed a theory of bordered Riemann surfaces. Riemann surfaces with bordered cusps we consider in the present paper are in fact bordered Riemann surfaces of [25, 24] with cusp decorations by horocycles (also introduced in [24]). However, our description of λ -lengths in terms of the extended shear coordinates that enables us to quantize the formers seems to be new. So, let us present the list of similarities/differences between our approach and that of Fomin, Shapiro, and Thurston:

- (i) Our arcs are *ordinary arcs* between decorated bordered cusps in the terminology of [24]; related ideal triangulations comprising only compatible ordinary arcs (with all punctures enclosed in monogons) are our CGL_a^{\max} .
- (ii) Our (exponentiated) extended shear coordinate $e^{\pi j}$ associated with the j th cusps is reciprocal to the L_r from [24], which is the length of the horocycle segment cut out by the corresponding ideal triangle.
- (iii) We always add to an ideal triangulation system arcs between neighboring cusps (excluded in [25, 24]). These arcs never mutate, correspond to frozen variables in the quantum cluster algebra case, but they are not central in the sense of Poisson or quantum algebra having nontrivial commutation relations with ordinary arcs and between themselves.

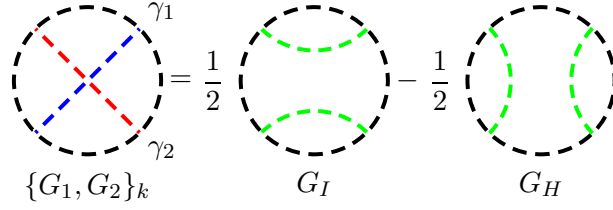


FIGURE 15. The “elementary” Poisson bracket (the Goldman bracket) $\{G_1, G_2\}_k$ (4.14) between two geodesic functions of the two corresponding curves γ_1 and γ_2 at their k th intersection point inside a Riemann surface: the curves and CGLs here are the same as in Fig. 14.

- (iv) In our treatment, we consider *only* triangulations by ordinary arcs (thus avoiding tagging and notching issues, which were crucial in [25, 24]). In fact, we can introduce shear coordinates for *any* fat graph $\mathcal{G}_{g,s,n} \in \Gamma_{g,s,n}$ dual to the corresponding partition of $\Sigma_{g,s,n}$ into ideal triangles whose sides are both tagged and ordinary arcs in the terminology of [25, 24]. Then the Poisson and quantum algebras of the shear coordinates on $\mathcal{G}_{g,s,n}$ will be given by the same formulas (Theorems 4.3 and 5.1 below) as for any fat graph $\hat{\mathcal{G}}_{g,s,n} \in \hat{\Gamma}_{g,s,n}$ and we can again express both λ -lengths of ordinary arcs and geodesic functions of closed curves in terms of these shear coordinates (using exactly the same combinatorial rules as before) thus obtaining the corresponding Poisson and quantum algebras (which, of course, retain their forms). We cannot however express λ -lengths of tagged arcs in terms of shear coordinates of $\mathcal{G}_{g,s,n}$ because these shear coordinates are insensitive to the tagging and to horocycle decorations corresponding to the tagging. We are therefore lacking Poisson and quantum algebras of tagged arcs. A possible reason hindering the very existence of Poisson and quantum algebras of tagged arcs compatible with the surface orientation is that, unlike ordinary arcs, we have only cyclic, not linear, ordering of tagged arcs winding to a hole/approaching a puncture, so, presumably, no decoration-free notion of a Poisson or quantum algebra exists for tagged arcs. In what follows, we thus consider only a sub-groupoid of MCG transformations that preserve the “monogon” property and are described by the generalized cluster algebra mutations of [14]; in reward we can explicitly quantize λ -lengths of the *ordinary arcs* from CGL_a^{\max} dual to corresponding fat graphs $\hat{\mathcal{G}}_{g,s,n} \in \hat{\Gamma}_{g,s,n}$ thus obtaining quantum cluster algebras of geometric type (see Sec. 5).

4.6. Goldman brackets for CGLs. We now introduce the Goldman bracket on the CGLs comprising closed curves and arcs (λ -lengths). For this, we introduce the Poisson relations for intersecting curves entering CGLs. Curves (either closed curves or arcs) can intersect either in the interior of the Riemann surface or at bordered cusps (if they are arcs incident to the same cusp(s)).

Let us define the *local resolution* $\{G_1, G_2\}_k$ at the k th intersection point p_k of two curves γ_1 and γ_2 . When p_k is an internal point of the surface, we set (see Fig. 15)

$$(4.14) \quad \{G_1, G_2\}_k = \frac{1}{2}G_I - \frac{1}{2}G_H,$$

where G_I and G_H are the same resolutions of the crossing as in the skein relation in Fig. 14

When two arcs meet at the same bordered cusp, the Goldman bracket between their geodesic functions at this cusp depends on the ordering of the corresponding arcs w.r.t. the orientation of the Riemann surface (see Fig. 16) ($G_1 = G_{a_1}$ and $G_2 = G_{a_2}$)

$$(4.15) \quad \{G_1, G_2\}_k = \pm \frac{1}{4}G_1G_2 := \begin{cases} \frac{1}{4}G_I & \text{if } a_1 \text{ is to the right of } a_2 \\ -\frac{1}{4}G_H & \text{if } a_1 \text{ is to the left of } a_2 \end{cases}$$

where we have the plus sign if the arc a_1 lies to the right from the arc a_2 when looking “from inside” the Riemann surface and minus sign if the arc a_1 lies to the left from the arc a_2 . Note that, since every arc has two ends, we must evaluate the brackets (4.15) for all four combinations of these ends (ends at different cusps Poisson commute); for instance, in the case where all four ends are at the same cusp,

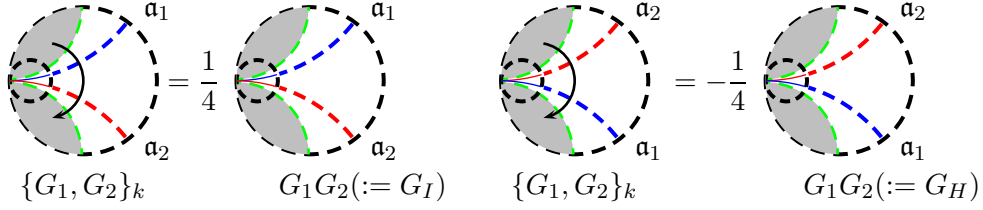


FIGURE 16. The “elementary” Poisson bracket (the Goldman bracket) $\{G_1, G_2\}_k$ (4.14) between two geodesic functions of the two corresponding arcs \mathfrak{a}_1 and \mathfrak{a}_2 coming to the same bordered cusp of a Riemann surface: the sign depends on the ordering of ends of the corresponding curves w.r.t. the orientation of the Riemann surface (indicated by an arrow).

and the both ends of \mathfrak{a}_1 are to the right of both ends of \mathfrak{a}_2 (provided these arcs has no intersections inside the Riemann surface), the total bracket will be $\{G_{\mathfrak{a}_1}, G_{\mathfrak{a}_2}\} = G_{\mathfrak{a}_1} G_{\mathfrak{a}_2}$.

The Poisson bracket (the Goldman bracket) between two geodesic laminations CGL_1 and CGL_2 (which may comprise both closed curves and arcs) with the set Q of intersection points p_k (for two arcs $\mathfrak{a}_l^{(1)} \in \text{CGL}_1$ and $\mathfrak{a}_m^{(2)} \in \text{CGL}_2$, we count intersections separately for every pair of endpoints of $\mathfrak{a}_l^{(1)}$ and $\mathfrak{a}_m^{(2)}$) is then geometrically defined to be

$$(4.16) \quad \{\text{CGL}_1, \text{CGL}_2\} = \sum_k \sum_{Q \setminus p_k} c_{\{I, H\}} \text{CGL}_{HIII\{I, H\}IHH\ldots}^{k\text{th}},$$

where $c_{\{I\}} = 1/2$ or $1/4$ and $c_{\{H\}} = -1/2$ or $-1/4$ depending on whether the point p_k is an inner point or a bordered cusp and we take the sum over all resolutions of the corresponding intersection of CGLs. Again, if in the process of resolution we obtain an empty closed loop, we assign the factor -2 to it; if we obtain an empty loop starting and terminating at the bordered cusp, we assign zero to it killing the corresponding $\text{CGL}_{HIII\{I, H\}I\ldots}$.

Lemma 4.2. *The semiclassical algebra of CGLs with the product defined in (4.9) and the Poisson bracket defined by (4.16) satisfies the classical Whitehead moves and semiclassical Jacobi relations.*

We postpone the *proof* till Sec. 5 where the above two cases will be corollaries of the quantum skein relations (they arise as the respective terms of orders \hbar^0 and \hbar^1 in the \hbar -expansion of the quantum Whitehead moves).

4.7. Poisson brackets for shear variables of bordered cusped Riemann surfaces. We now introduce the Poisson bivector field (the Poisson bracket) on $\widehat{\mathfrak{T}}_{g,s,n}^H$ that is invariant w.r.t. morphisms of $\widehat{\mathfrak{T}}_{g,s,n}^H$.

Theorem 4.3. *In the coordinates Z_α of $\widehat{\mathfrak{T}}_{g,s,n}^H$ on any fixed spine $\widehat{\mathcal{G}}_{g,s,n} \in \widehat{\Gamma}_{g,s,n}$ corresponding to a surface with at least one bordered cusp, the Weil–Petersson bracket B_{WP} reads*

$$(4.17) \quad \{f(\mathbf{Z}), g(\mathbf{Z})\} = \sum_{\substack{3\text{-valent} \\ \text{vertices } \alpha=1}}^{4g+2s+|\delta|-4} \sum_{i=1}^{3 \bmod 3} \left(\frac{\partial f}{\partial Z_{\alpha_i}} \frac{\partial g}{\partial Z_{\alpha_{i+1}}} - \frac{\partial g}{\partial Z_{\alpha_i}} \frac{\partial f}{\partial Z_{\alpha_{i+1}}} \right),$$

where the sum ranges all three-valent vertices of a graph that are not adjacent to loops and α_i are the labels of the cyclically (clockwise) ordered ($\alpha_4 \equiv \alpha_1$) edges (irrespectively whether inner or outer) incident to the vertex with the label α . This bracket

- (1) is equivariant w.r.t. the morphisms generated by flips (mutations) of inner edges described by formula (2.11) and by flips (mutations) of edges adjacent to loops described by Lemma 2.3;
- (2) gives rise to the Goldman bracket (4.16) on the space of CGLs [31].

The centre of this Poisson algebra is a linear span of $\sum_{\alpha \in I} Z_\alpha$ where we take the sum (with proper multiplicities) over indices of edges bounding a cusped hole (labeled I). Recall that coefficients ω_j of monogons are central by construction. These coefficients are either $2 \cosh(P_j/2)$, where P_j are perimeters of holes that do not contain bordered cusps, or $2 \cos(\pi/p_j)$, where $p_j \in \mathbb{Z}_{\geq 2}$ are orders of orbifold points. The dimension of the centre is obviously s_{h_1} , that is, the number of holes with nonzero number of bordered cusps, and the total dimension of any Poisson leaf of $\widehat{\mathfrak{T}}_{g,s,n}^H$ is $6g - 6 + 2s + 2n$. The Poisson dimension is therefore even and it is positive only for stable curves.

We just outline the proof because we can consider it a corollary of the corresponding statement in the quantum case. Proving the preservation of Poisson brackets is easy (and in fact was already done in Sec. 2 because we do not enlarge the set of mutations: we are not allowed to mutate open edges). The strategy of proving that the brackets (4.17) imply the Goldman brackets is based on the invariance of products of matrices under the trace signs under the flip morphisms (formulas (2.12)–(2.14) and (2.17)–(2.19)). Using MCG transformations, we can then reduce the intersection pattern between two curves in two CGLs to a handful of cases, each of which admits a local (quantum) resolution presented in the next section.

We next address the problem of Poisson relations between λ -lengths of arcs belonging to the same CGL. In order to describe these Poisson brackets we need to introduce one more notation. Given a CGL_a^{\max} , let us enumerate arcs of this lamination as follows. We first introduce the index $s = 1, \dots, n$ enumerating all bordered cusps of $\Sigma_{g,s,n}$. At every cusp we have $r_s \geq 2$ ends of arcs from the CGL_a^{\max} terminating at this cusp. We have a prescribed linear ordering on the set of these ends coming from the CGL_a^{\max} , so we enumerate these ends by a subindex $i = 1, \dots, r_s$ (these sets of ends are always nonempty as we always include bordering arcs into every CGL_a^{\max}) and set $s_i < s_j$ if $i < j$. Every arc of the lamination can be then indexed by labels of its ends, s_i and t_j , and we denote its λ -length by λ_{s_i, t_j} .

Corollary 4.4. *Because λ -lengths λ_{s_i, t_j} and λ_{p_l, q_k} of arbitrary two arcs from the same CGL_a^{\max} admit monomial representations in terms of the extended shear coordinates of the fat graph $\widehat{\mathcal{G}}_{g,s,n}$ dual to CGL_a^{\max} (see Proposition 4.1), Poisson relations for these shear coordinates (4.17) imply homogeneous Poisson relations between λ_{s_i, t_j} and λ_{p_l, q_k} . These relations read*

$$\{\lambda_{s_i, t_j}, \lambda_{p_l, q_k}\} = \lambda_{s_i, t_j} \lambda_{p_l, q_k} \left[\frac{\varepsilon_{i-l} \delta_{s,p} + \varepsilon_{j-l} \delta_{t,p} + \varepsilon_{i-k} \delta_{s,q} + \varepsilon_{j-k} \delta_{t,q}}{4} \right] := \lambda_{s_i, t_j} \lambda_{p_l, q_k} I(\mathbf{a}_1, \mathbf{a}_2)/4, \quad \varepsilon_k := \text{sign}(k), \quad (4.18)$$

where $I(\mathbf{a}_1, \mathbf{a}_2)$ is the incidence index of two arcs that do not intersect inside the Riemann surface.

4.8. Poisson algebras of geodesic functions in the case of no bordered cusps. Let us explain here how to fully characterise the Poisson algebra of geodesic functions on a Riemann surface $\Sigma_{g,s}$ for any genus g and any number $s_h > 1$ of holes and any number of s_o of orbifold points ($s = s_o + s_h$) as a specific Poisson sub-algebra of the set of geodesics functions and arcs on $\tilde{\Sigma}_{g,s,1}$ i.e. a Riemann surface with the same genus g , the same number $s_h > 1$ of holes and the same number of s_o of orbifold points with at least one bordered cusp on one of the holes.

For simplicity let us restrict to the case when there are no orbifold points, so that $s_h = s$. The general case can be done in the same way.

The Teichmüller space for $\Sigma_{g,s}$ is $\mathbb{R}^{6g-6+2s} \times \Omega^s$, while for $\tilde{\Sigma}_{g,s,1}$ is $\mathbb{R}^{6g-6+2s+3} \times \Omega^{s-1}$ because we have $s-1$ holes with no cusps and $s_{h_1} = 1$ holes with 1 cusp on it.

The Riemann surface $\tilde{\Sigma}_{g,s,1}$ is laminated by $s-1$ closed geodesics around the non-cusped holes and by $6g - 6 + 2s + 3$ arcs. The Poisson algebra is therefore of dimension $6g - 6 + 3s + 2$ and admits s central elements - the $s-1$ lengths of the closed geodesics around the non-cusped holes and the λ -length of the arc that follows the fat graph starting from the cusp, going always left until it ends at the cusp again.

Let us now consider the closed geodesic g around the cusped hole (homeomorphic to the closed path going exactly around the hole and separating its part with the cusp from the rest of the surface) and take the set \mathcal{F}_g of all functions of the lamination that Poisson commute with it. This forms a closed Poisson algebra due to the following simple lemma.

Lemma 4.5. *Given a Poisson algebra $(\mathcal{A}, \{\cdot, \cdot\})$ and any element $g \in \mathcal{A}$, the set $\mathcal{F} = \{f \in \mathcal{A} \mid \{f, g\} = 0\}$ is a Poisson sub-algebra with the induced Poisson bracket.*

Proof. The statement is a trivial consequence of the Jacobi identity. \square

The Poisson algebra \mathcal{F}_g coincides with the Poisson algebra of geodesic functions on the Riemann surface $\Sigma_{g,s}$ by construction and has dimension $6g - 6 + 3s + 1$ with $s + 1$ Casimirs.

Example 4.12. Let us illustrate the procedure in the case of a torus with one hole $\Sigma_{1,1}$. In this case the fat-graph is given by a prezzle (see Fig. 4.12) and the Poisson algebra is generated by the lengths of the three simple closed geodesics going along two edges: $G_{Z_1 Z_0}$, $G_{Z_2 Z_1}$, $G_{Z_0 Z_2}$ which satisfy the following Poisson relations:

$$\begin{aligned} \{G_{Z_2 Z_1}, G_{Z_1 Z_0}\} &= \frac{1}{2} G_{Z_2 Z_1} G_{Z_1 Z_0} - G_{Z_0 Z_2}, \\ \{G_{Z_1 Z_0}, G_{Z_0 Z_2}\} &= \frac{1}{2} G_{Z_1 Z_0} G_{Z_0 Z_2} - G_{Z_2 Z_1}, \\ \{G_{Z_0 Z_2}, G_{Z_2 Z_1}\} &= \frac{1}{2} G_{Z_0 Z_2} G_{Z_2 Z_1} - G_{Z_1 Z_0}, \end{aligned}$$

with central element:

$$G_{Z_2 Z_1}^2 + G_{Z_1 Z_0}^2 + G_{Z_0 Z_2}^2 - G_{Z_2 Z_1} G_{Z_1 Z_0} G_{Z_0 Z_2}.$$

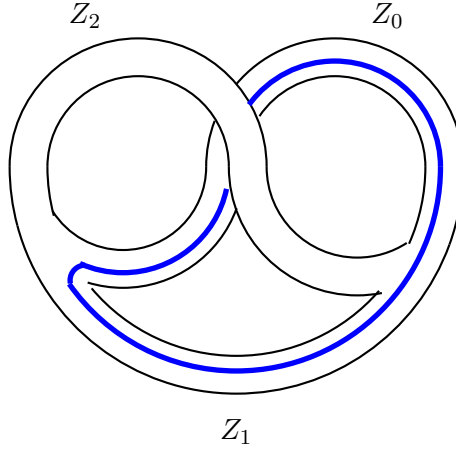


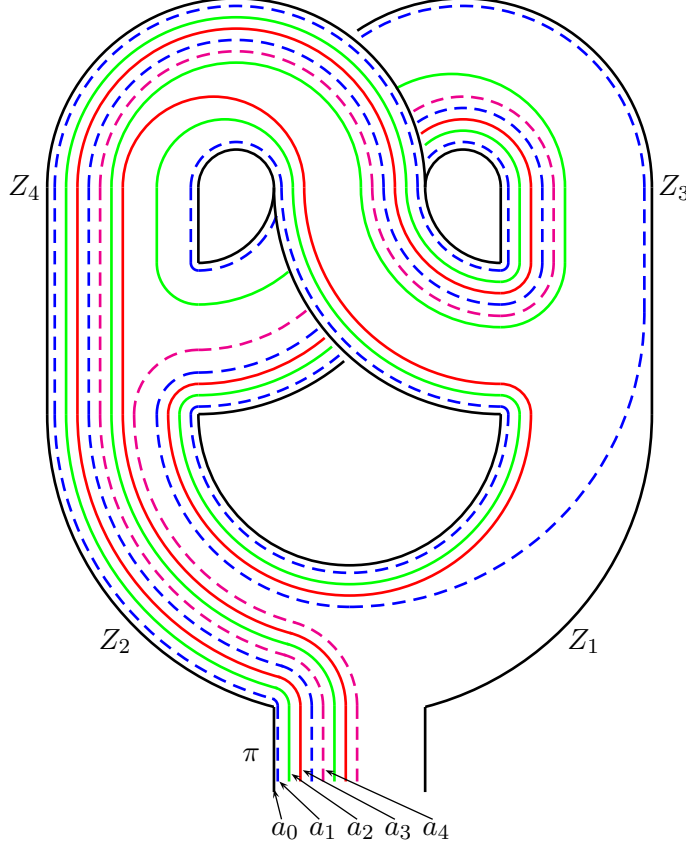
FIGURE 17. Fat-graph of $\Sigma_{1,1}$ with the geodesic $G_{Z_1 Z_0}$ in blue.

Let us now characterise this algebra as a sub-algebra of the algebra given by the lamination of a torus with one hole and one cusp on the hole $\tilde{\Sigma}_{1,1,1}$. The fat-graph in this case is given in Fig. 18.

We choose the lamination in the canonical form from Proposition 4.1 (in this form, all arcs are monomials in the exponentiated shear coordinates).

The elements constituting the lamination are:

$$(4.19) \quad \begin{aligned} a_0 &= e^{\pi + Z_1 + Z_2 + Z_3 + Z_4}, & a_1 &= e^{\pi + Z_1 + 2Z_2 + \frac{3}{2}Z_3 + \frac{3}{2}Z_4}, & a_2 &= e^{\pi + \frac{1}{2}Z_1 + \frac{3}{2}Z_2 + Z_3 + \frac{3}{2}Z_4}, \\ a_3 &= e^{\pi + \frac{1}{2}Z_1 + \frac{3}{2}Z_2 + \frac{1}{2}Z_3 + Z_4}, & a_4 &= e^{\pi + Z_2 + \frac{1}{2}Z_3 + \frac{1}{2}Z_4}, \end{aligned}$$

FIGURE 18. The (canonical) system of arcs for $\Sigma_{1,1,1}$.

where a_0 is central. Note that because the above relations are invertible, we can equivalently express all shear coordinates in terms of arcs using formulas (2.3) and (4.2):

$$(4.20) \quad \begin{aligned} e^\pi &= \frac{a_0 a_4}{a_1}, & e^{Z_1} &= \frac{a_0 a_3}{a_2 a_4}, & e^{Z_2} &= \frac{a_1 a_3}{a_0 a_2}, \\ e^{Z_3} &= \frac{a_1 a_4}{a_3^2}, & e^{Z_4} &= \frac{a_2^2}{a_1 a_4}. \end{aligned}$$

Let us now consider the closed geodesic around the hole:

$$g = \text{tr}(RX_{Z_1}LX_{Z_3}LX_{Z_4}LX_{Z_1}LX_{Z_2}LX_{Z_3}LX_{Z_4}LX_{Z_2}).$$

It is straightforward to verify that the set of functions that Poisson commute with g is generated by $g, a_0, \frac{a_1}{a_2}, \frac{a_2}{a_3}, \frac{a_3}{a_4}$. The three simple closed geodesics of the uncusped case now correspond to:

$$G_1 = \text{tr}(LX_{Z_2}RX_{Z_4}LX_{Z_1}), \quad G_2 = \text{tr}(LX_{Z_2}LX_{Z_3}RX_{Z_1}), \quad G_3 = \text{tr}(LX_{Z_4}RX_{Z_3}).$$

We can express these in terms of the lamination as follows:

$$\begin{aligned} G_1 &= \frac{a_4}{a_3} + \frac{a_3}{a_4} + \frac{a_2^2}{a_1 a_3} + \frac{a_0 a_2}{a_1 a_4}, \\ G_2 &= \frac{a_2}{a_1} + \frac{a_1}{a_2} + \frac{a_3^2}{a_2 a_4} + \frac{a_0 a_3}{a_1 a_4}, \\ G_3 &= \frac{a_2}{a_3} + \frac{a_3}{a_2} + \frac{a_1 a_4}{a_2 a_3}. \end{aligned}$$

It is straightforward to see that G_1, G_2, G_3 and g generate the sub-algebra of all functions of a_0, \dots, a_4 that Poisson commute with g and that these geodesic functions satisfy the Poisson relations

$$\{G_1, G_2\} = \frac{1}{2}G_1G_2 - G_3, \quad \{G_2, G_3\} = \frac{1}{2}G_2G_3 - G_1, \quad \{G_3, G_1\} = \frac{1}{2}G_3G_1 - G_2,$$

with the central element

$$G_1 G_2 G_3 - G_1^2 - G_2^2 - G_3^2.$$

This central element is equal to $2 - g$.

5. QUANTUM ALGEBRAS

5.1. Quantum algebras of arcs. We first start with quantising Poisson relations for shear coordinates on Riemann surfaces with bordered cusps. We have the quantum analogue of Theorem 4.3.

Theorem 5.1. *Introducing the Hermitian operators Z_α^h corresponding to the coordinates Z_α of $\widehat{\mathfrak{T}}_{g,s,n}^H$ on any fixed spine $\widehat{\mathcal{G}}_{g,s,n} \in \widehat{\Gamma}_{g,s,n}$, the commutation relations between these operators are given by the formula*

$$(5.21) \quad [Z_\alpha^h, Z_\beta^h] = 2\pi i \hbar \{Z_\alpha, Z_\beta\},$$

where $\{Z_\alpha, Z_\beta\}$ are the Poisson brackets given by the formula (4.17). These commutation relations

- (1) are equivariant w.r.t. the quantum flip morphisms generated by flips (mutations) of inner edges described by formula (2.23) and by flips (mutations) of edges adjacent to loops described by Lemma 2.6;
- (2) gives rise to the quantum skein relations on the space of CGLs [31].

The Casimirs of these quantum algebras are again $\sum_{\alpha \in I} Z_\alpha^h$ where we take the sum (with proper multiplicities) over indices of edges bounding a cusped hole (labeled I).

Whereas no obvious natural ordering of quantum shear coordinates entering a quantum geodesic function for a closed geodesic exists, it appears that we have one for quantum shear coordinates of arcs.

Lemma 5.2. *The quantum ordering that*

- (1) is preserved by the quantum flip morphisms in (2.23) and in Lemma 2.6 and
- (2) ensures that all geodesic arcs are Hermitian operators

is the natural quantum ordering (coinciding with the ordering of matrix product) provided we replace $R \rightarrow q^{-1/4}R$ and $L \rightarrow q^{1/4}L$ at all their appearances.

The **proof** is based on formulas (2.25)–(2.27) and (2.30)–(2.32) using which we can reduce *any* arc to one of the following cases:

- (1) if an arc starts and terminates at different bordered cusps labeled 1 and 2, then we have either $\text{tr}[KX_{\pi_2}Rq^{-1/4}X_{\pi_1}]$ with $[\pi_2, \pi_1] = 2\pi i \hbar$ or $\text{tr}[KX_{\pi_2}LX_YRX_{\pi_1}]$ with $[Y, \pi_2] = [Y, \pi_1] = 2\pi i \hbar$, $[\pi_1, \pi_2] = 0$; a direct calculation in the both cases demonstrate that these expressions are Hermitian operators.
- (2) if an arc starts and terminates at the same bordered cusp, then we have either

$$\text{tr}[KX_\pi RX_Y F_\omega X_Y LX_\pi], \quad [Y, \pi] = 2\pi i \hbar,$$

or

$$q^{-1/4} \text{tr}[KX_\pi RX_{Y_1} LX_{Y_2} RX_\pi], \quad [Y_1, \pi] = [Y_1, Y_2] = [\pi, Y_2] = 2\pi i \hbar$$

or

$$q^{-1/2} \text{tr}[KX_\pi RX_{Y_1} RX_{Y_2} LX_{Y_3} RX_\pi], \quad [Y_1, \pi] = [Y_2, Y_1] = [Y_2, Y_3] = [\pi, Y_3] = 2\pi i \hbar$$

All these expressions with the natural ordering of quantum entries are Hermitian operators.

Lemma 5.3. *All quantum arcs from the same quantum CGL have homogeneous (q -commutation) relations:*

$$(5.22) \quad q^{I(\mathbf{a}_1, \mathbf{a}_2)/4} G_{\mathbf{a}_1}^h G_{\mathbf{a}_2}^h = q^{-I(\mathbf{a}_1, \mathbf{a}_2)/4} G_{\mathbf{a}_2}^h G_{\mathbf{a}_1}^h,$$

where $I(\mathbf{a}_1, \mathbf{a}_2) = -I(\mathbf{a}_2, \mathbf{a}_1)$ is the “incidence index” (4.18) of two arcs \mathbf{a}_1 and \mathbf{a}_2 that have no intersections inside the Riemann surface. Recall that this index can take values $-4, -2, -1, 0, 1, 2, 4$.

The **proof** again uses the invariance of quantum arcs w.r.t. quantum flip morphisms. Using this invariance we can again reduce the pattern to one of a finite number of cases. We can then verify the quantum skein relations (5.22) at each case separately.

5.2. Quantum skein relations for arcs. As we have seen in sub-section 4.3, in order for the skein relation (4.3) to make sense geometrically, we need to cyclically permute the factors that form the matrices A and B . When we are dealing with the quantum case, the entries of these matrices no longer commute, so that cyclic permutations bring in some q -factors.

Let us consider a specific example (see Fig. 19) with two quantum arcs intersecting once:

$$(5.23) \quad G_1^h = \text{tr}(\cdots X_{T_2} L X_{T_1} R X_T L X_Z R X_X L X_{X_1} R X_{X_2} \cdots) \text{ and } G_2^h = \text{tr}(\cdots X_P R X_Z L X_Y \cdots).$$

We use that

$${}^1X_X {}^2X_Y = {}^2X_Y {}^1X_X Q = {}^2X_Y Q^{-1} {}^1X_X.$$

We then push the second arc in (5.23) from the right through the first arc until two insertions of X_Z will become neighbour (this is to make sure that all quantities involved in our quantum skein relation indeed describe quantum arcs). We obtain

$$(5.24) \quad G_1^h G_2^h = \text{tr}_{12} \left(\cdots {}^1X_{T_2} {}^1L {}^1X_{T_1} {}^1R {}^1X_T {}^1L {}^2X_P {}^1X_Z Q^{-1} {}^2R {}^2X_Z \bullet {}^1R {}^1X_X Q^{-1} {}^2L {}^2X_Y {}^1L {}^1X_{X_1} {}^1R {}^1X_{X_2} \cdots \right)$$

where the bullet is the place where we are going to insert $\mathbb{I} \times \mathbb{I}$ like in the classical case. We now however have to replace the classical matrices P_{12} and \tilde{P}_{12} by their quantum analogues.

Let us start from the quantum analogue \tilde{r}_{12} of $-\tilde{P}_{12}$:

$$(5.25) \quad \tilde{r}_{12} := q {}^1e_{22} \otimes {}^2e_{11} + q^{-1} {}^1e_{11} \otimes {}^2e_{22} - {}^1e_{12} \otimes {}^2e_{21} - {}^1e_{21} \otimes {}^2e_{12},$$

or

$$\tilde{r}_{12} = \begin{bmatrix} 0 & 0 & 0 & 0 \\ 0 & q^{-1} & -1 & 0 \\ 0 & -1 & q & 0 \\ 0 & 0 & 0 & 0 \end{bmatrix}.$$

It is straightforward to verify that

$$\begin{aligned} \tilde{r}_{12} ({}^1R {}^1X_S \otimes {}^2\mathbb{E}) Q^{-1} &= q^{1/2} \tilde{r}_{12} ({}^1\mathbb{E} \otimes {}^2X_S L), \\ \tilde{r}_{12} ({}^1L {}^1X_S \otimes {}^2\mathbb{E}) Q &= q^{-1/2} \tilde{r}_{12} ({}^1\mathbb{E} \otimes {}^2X_S R), \\ Q^{-1} ({}^1X_S R \otimes {}^2\mathbb{E}) \tilde{r}_{12} &= q^{1/2} ({}^1\mathbb{E} \otimes {}^2L {}^1X_S) \tilde{r}_{12}, \\ Q ({}^1X_S L \otimes {}^2\mathbb{E}) \tilde{r}_{12} &= q^{-1/2} ({}^1\mathbb{E} \otimes {}^2R {}^1X_S) \tilde{r}_{12}, \end{aligned}$$

that is, \tilde{r}_{12} is indeed the quantum analogue of $-\tilde{P}_{12}$.

We now define the quantum analogue r_{12} of P_{12} . This is defined as

$$(5.26) \quad r_{12} = q {}^1\mathbb{I} \otimes {}^2\mathbb{I} - \tilde{r}_{12},$$

so that

$$r_{12} = \begin{bmatrix} q & 0 & 0 & 0 \\ 0 & q - q^{-1} & 1 & 0 \\ 0 & 1 & 0 & 0 \\ 0 & 0 & 0 & q \end{bmatrix}.$$

Observe that $r_{12} = -q^{\frac{1}{2}} s_{12} P_{12}^q$ where

$$(5.27) \quad P_{12}^q = \begin{bmatrix} 1 & 0 & 0 & 0 \\ q - 1 & q - q^{-1} & 1 & 0 \\ 0 & 1 & 0 & 0 \\ 0 & q^{-1} - 1 & 0 & 1 \end{bmatrix},$$

and

$$(5.28) \quad s_{12} = \overset{1}{L} Q^{-1} \overset{1}{R} = \begin{bmatrix} -q^{1/2} & 0 & 0 & 0 \\ q^{1/2} - q^{-1/2} & -q^{-1/2} & 0 & 0 \\ 0 & 0 & -q^{-1/2} & 0 \\ 0 & 0 & q^{-1/2} - q^{1/2} & -q^{1/2} \end{bmatrix}.$$

These two matrices satisfy the following useful properties:

$$P_{12}^q \overset{1}{R} Q \overset{2}{L} Q = P_{12} \overset{1}{R} \otimes \overset{2}{L},$$

and

$$\overset{2}{X}_Z s_{12} \overset{1}{L} \overset{1}{X}_Y = \overset{1}{L} \overset{1}{X}_Y \otimes \overset{2}{X}_Z = \overset{1}{L} \overset{2}{X}_Z Q^{-1} \overset{1}{X}_Y,$$

so that s_{12} to effectively permutes $\overset{2}{X}_Z$ and $\overset{1}{X}_Y$.

Let us now insert $q\mathbb{I} \times \mathbb{I} = r_{12} + \tilde{r}_{12}$ in (5.24) and see the effect of \tilde{r}_{12} (the case of r_{12} is easier and we leave it to the reader: one just have to check that all matrices Q appearing when pushing matrices X one through another are indeed killed by r_{12}). On the left of \tilde{r}_{12} , we then obtain that

$$\begin{aligned} \tilde{r}_{12} \overset{1}{R} \overset{1}{X}_X Q^{-1} \overset{2}{L} \overset{2}{X}_Y \overset{1}{L} \overset{1}{X}_{X_1} \overset{1}{R} \overset{1}{X}_{X_2} \cdots &= q^{1/2} \tilde{r}_{12} \overset{2}{X}_X \overset{2}{L} \overset{2}{L} \overset{2}{X}_Y \overset{1}{L} \overset{1}{X}_{X_1} \overset{1}{R} \overset{1}{X}_{X_2} \cdots \\ &= -q^{1/2} \tilde{r}_{12} \overset{1}{L} \overset{1}{X}_{X_1} Q \overset{2}{X}_X \overset{2}{L} \overset{2}{X}_Y \overset{1}{L} \overset{1}{X}_{X_2} \cdots = -\tilde{r}_{12} \overset{2}{X}_{X_1} \overset{2}{R} \overset{2}{L} \overset{2}{X}_{X_2} \overset{2}{X}_X \overset{2}{L} \overset{2}{X}_Y \cdots \\ &= -\tilde{r}_{12} \overset{1}{R} \overset{1}{X}_{X_2} Q^{-1} \overset{2}{X}_{X_1} \overset{2}{L} \overset{2}{X}_X \overset{2}{L} \overset{2}{X}_Y \cdots = -q^{1/2} \tilde{r}_{12} \overset{2}{X}_{X_2} \overset{2}{L} \overset{2}{X}_{X_1} \overset{2}{R} \overset{2}{X}_X \overset{2}{L} \overset{2}{X}_Y \cdots, \end{aligned}$$

so the action of \tilde{r}_{12} inverts the order of quantum operators entering a quantum arc. This happens on the left side of \tilde{r}_{12} as well: the first action however happens in “opposite” order, we use that

$$\overset{1}{L} \overset{1}{X}_Z Q^{-1} \overset{2}{R} \overset{2}{X}_Z \tilde{r}_{12} = q^{12} \overset{1}{L} \overset{1}{X}_Z \overset{1}{X}_Z \overset{1}{L} \tilde{r}_{12} = q^{12} \overset{1}{R} \tilde{r}_{12}$$

to present the expression to the left from \tilde{r}_{12} as

$$\begin{aligned} q^{1/2} \cdots \overset{1}{X}_{T_2} \overset{1}{L} \overset{1}{X}_{T_1} \overset{1}{R} \overset{1}{X}_T \overset{1}{R} \overset{1}{X}_P \tilde{r}_{12} &= q^{1/2} \cdots \overset{1}{X}_{T_2} \overset{1}{L} \overset{1}{X}_{T_1} \overset{1}{R} \overset{1}{X}_P Q^{-1} \overset{1}{X}_T \overset{1}{R} \tilde{r}_{12} \\ &= q \cdots \overset{1}{X}_{T_2} \overset{1}{L} \overset{1}{X}_{T_1} \overset{1}{R} \overset{1}{X}_P \overset{2}{L} \overset{2}{X}_T \tilde{r}_{12} = q \cdots \overset{1}{X}_{T_2} \overset{1}{L} \overset{1}{X}_P \overset{2}{L} \overset{2}{X}_T Q^{-1} \overset{1}{X}_{T_1} \overset{1}{R} \tilde{r}_{12} \\ &= q^{3/2} \cdots \overset{1}{X}_{T_2} \overset{1}{L} \overset{1}{X}_P \overset{2}{L} \overset{2}{X}_T \overset{2}{R} \overset{2}{X}_{T_1} \tilde{r}_{12} = q^{3/2} \cdots \overset{2}{X}_P \overset{2}{L} \overset{2}{X}_T \overset{2}{R} \overset{2}{X}_{T_1} Q \overset{1}{X}_{T_2} \overset{1}{L} \tilde{r}_{12} \\ &= q \cdots \overset{2}{X}_P \overset{2}{L} \overset{2}{X}_T \overset{2}{R} \overset{2}{X}_{T_1} \overset{2}{R} \overset{2}{X}_{T_2} \tilde{r}_{12}, \text{ etc.} \end{aligned}$$

As a result, we obtain two new arcs two halves of which are “reflected” from the insertion of \tilde{r}_{12} . We also see that the above reflections respect the following mnemonic law: if we multiply all R by $q^{-1/4}$ and all L by $q^{1/4}$, the q -factors will be absorbed into the definitions of R and L .

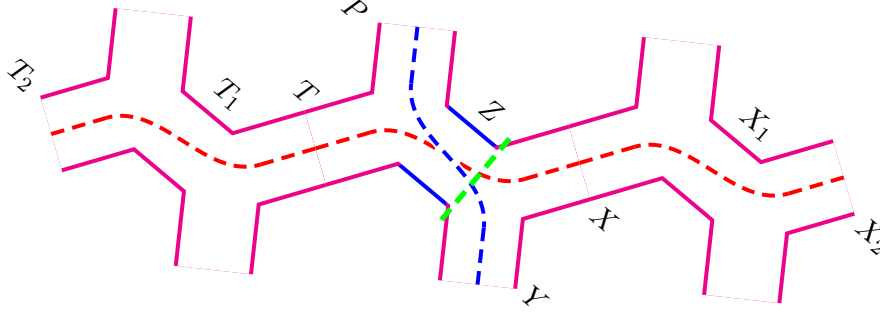


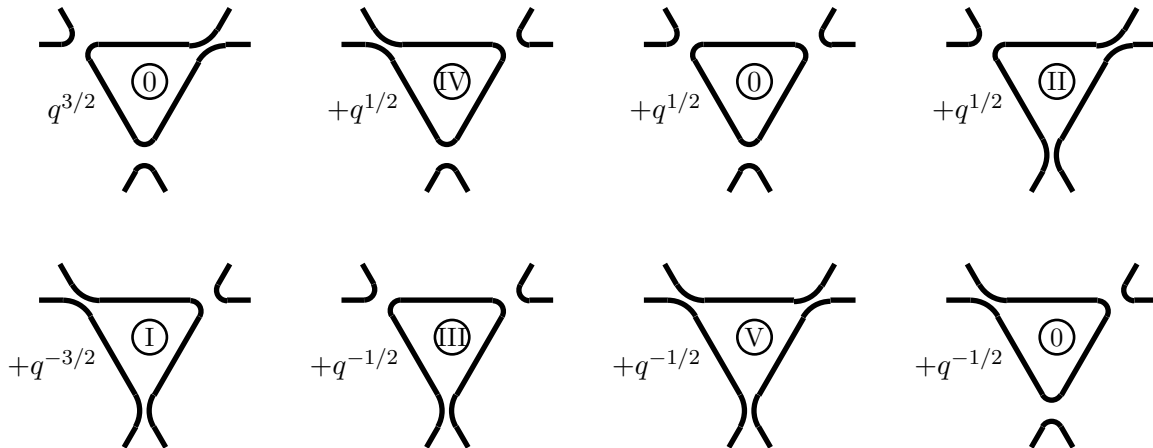
FIGURE 19. Example of a single arc intersection. The vertical dashed line indicates the position of insertions.

5.3. Riedemeister moves for quantum geodesic functions. For the case of CGL, we have three Riedemeister moves for quantum geodesic function algebras. The first two of them are standard, we present them only for the integrity of the presentation.

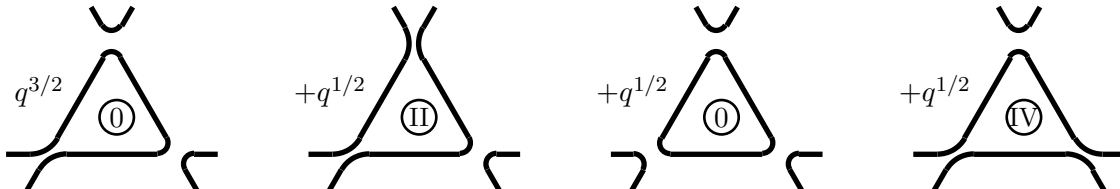
(i). Given three quantum geodesic functions G_i or quantum arcs (we do not distinguish between geodesic functions and arcs in this relation), we have

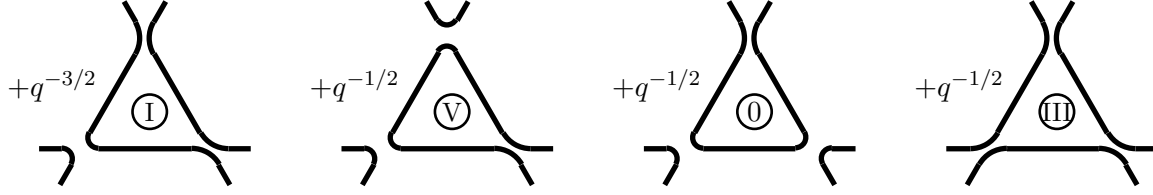
$$\begin{array}{c} G_2^h \\ \diagup \quad \diagdown \\ G_1^h \text{---} \text{---} G_3^h \end{array} = \begin{array}{c} G_2^h \\ \diagdown \quad \diagup \\ G_1^h \text{---} \text{---} G_3^h \end{array}$$

where the upper/lower crossing indicates the order of the corresponding terms in the quantum product: the both above formulas correspond to the same product $G_1^h G_2^h G_3^h$. We prove this identity by resolving all crossings in two possible ways. On each side we have eight diagrams: in the left-hand side we have:



and on the right-hand side we have





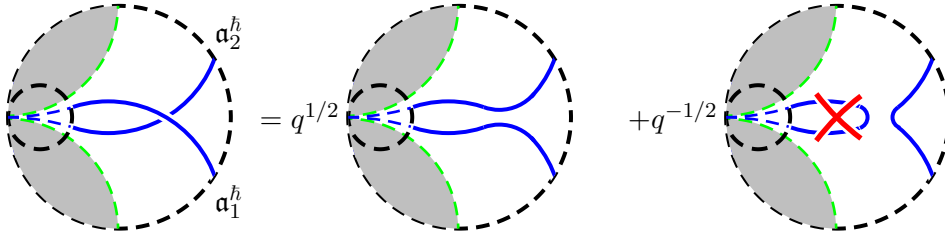
Here, for the convenience, we have indicated by Roman numerals homotopic terms in the both sides of the equality. The terms indicated by “0” labels cancel separately on the both sides of the equality provided we set the empty loop equal to $-q - q^{-1}$.

(ii). The second Riedemeister move reads

$$\frac{G_1^h}{G_2^h} = \frac{q}{\text{diagram}} + \frac{1}{\text{diagram}} + \frac{1}{\text{diagram}} + \frac{q^{-1}}{\text{diagram}} = \frac{G_1^h}{G_2^h}$$

Here, again, all unwanted terms labeled “0” are mutually canceled provided the empty loop is equal to $-q - q^{-1}$.

(iii). The new, third, Riedemeister move of two arcs terminating at the same cusp reads



where the second diagram kills the whole lamination if we set the empty loop starting and terminating at the same bordered cusp to be zero.

5.4. Quantum cluster algebras of geometric type. When quantizing the shear coordinates we associate to Z_α and π_j Hermitian operators Z_α^h, π_j^h with constant commutation relations (5.21).

We now fix a spine $\widehat{\mathcal{G}}_{g,s,n} \in \widehat{\Gamma}_{g,s,n}$. For any arc \mathbf{a} (not necessarily belonging to $\text{CGL}_\mathbf{a}^{\max}$ dual to $\widehat{\mathcal{G}}_{g,s,n}$) we define the quantum λ -length (geodesic function) to be

$$(5.29) \quad \lambda_\mathbf{a}^h := G_\mathbf{a} := \text{tr} [X_{\pi_{j_1}} \tilde{L} X_{Z_{\alpha_1}} \tilde{R} \dots X_{Z_j} F_{\omega_j} X_{Z_j} \dots X_{Z_{\alpha_n}} \tilde{R} X_{\pi_{j_2}} K],$$

where $\tilde{L} = q^{1/4} L$, $\tilde{R} = q^{-1/4} R$, the matrices F_ω and K are the same as in the classical case, and the quantum ordering of operators coincides with the natural ordering of the matrix product.

Theorem 5.4. *Let $\mathbb{Z}_{\geq 0}[(\lambda_\alpha^h)^{\pm 1}, q^{\pm 1/4}, \omega_j]$ be the ring of polynomials with nonnegative integer coefficients where λ_α^h are quantum λ -lengths comprising a $\text{CGL}_\mathbf{a}^{\max}$, so all relations are understood modulo equivalence relations*

$$q^{I(\mathbf{a}_1, \mathbf{a}_2)/4} \lambda_{\mathbf{a}_1}^h \lambda_{\mathbf{a}_2}^h = q^{-I(\mathbf{a}_1, \mathbf{a}_2)/4} \lambda_{\mathbf{a}_2}^h \lambda_{\mathbf{a}_1}^h,$$

assuming that q and ω_j commute with all variables.

Then the quantum λ -length of any other arc expressed in terms of shear coordinates by Lemma 5.2, belongs to $\mathbb{Z}_{\geq 0}[(\lambda_\alpha^h)^{\pm 1}, q^{\pm 1/4}, \omega_j]$ (the Laurentian and positivity property).

Vice versa, the shear coordinates determined by the spine $\widehat{\mathcal{G}}_{g,s,n} \in \widehat{\Gamma}_{g,s,n}$ dual to the above $\text{CGL}_{\mathbf{a}}^{\max}$ are monomials in quantum λ -variables; explicitly,

$$(5.30) \quad e^{Z_e^h/2} = q^{S/16} (\lambda_b^h)^{1/2} (\lambda_d^h)^{1/2} (\lambda_a^h)^{-1/2} (\lambda_c^h)^{-1/2}, \quad (\text{cf. Fig. 3}),$$

for internal edges that are not incident to loops; here

$$S = I(\mathbf{a}_b, \mathbf{a}_d) - I(\mathbf{a}_b, \mathbf{a}_a) - I(\mathbf{a}_b, \mathbf{a}_c) - I(\mathbf{a}_d, \mathbf{a}_a) - I(\mathbf{a}_d, \mathbf{a}_c) + I(\mathbf{a}_a, \mathbf{a}_b);$$

$$(5.31) \quad e^{Z_j^h} = q^{-I(\mathbf{a}_b, \mathbf{a}_a)/4} \lambda_b^h (\lambda_a^h)^{-1} \quad (\text{cf. Fig. 5})$$

for internal edges incident to loops, and

$$(5.32) \quad e^{\pi_j^h/2} = q^{R/16} (\lambda_c^h)^{1/2} (\lambda_b^h)^{1/2} (\lambda_a^h)^{-1/2} \quad (\text{cf. Fig. 13})$$

for external edges, where $R = I(\mathbf{a}_c, \mathbf{a}_b) - I(\mathbf{a}_c, \mathbf{a}_a) - I(\mathbf{a}_b, \mathbf{a}_a)$.

The proof is by construction: that $e^{Z_e^h/2}$, $e^{Z_j^h}$, and $e^{\pi_j^h/2}$ are monomials in the λ -variables entering the special $\text{CGL}_{\mathbf{a}}^{\max}$ dual to $\widehat{\mathcal{G}} \in \widehat{\Gamma}_{g,s,n}$ follows from geometry; powers of q follow from the Hermiticity property of quantum shear coordinates. The quantum λ -length $\lambda_{\mathbf{a}}$ corresponding to *any* arc \mathbf{a} (entering *some* $\text{CGL}_{\mathbf{a}}^{\max}$) is expressed by Lemma 5.2 as an ordered quantum polynomial in $e^{\pm Z_{\alpha}^h/2}$, $e^{\pm Z_j^h}$, $e^{\pi_j^h/2}$, and ω_j . All λ -lengths enter these expressions in integer, not half-integer, powers. To see this, let us consider the product of matrices in Lemma 5.2: disregarding left and right turns and ω_j , we have an (ordered) string of shear coordinates $\pi_{j_1}^h, Z_{\alpha_1}^h, \dots, Z_{\alpha_k}^h, Z_j^h, Z_j^h, Z_{\alpha_{k+1}}^h, \dots, Z_{\alpha_n}^h, \pi_{j_2}^h$ (cf. expression (5.29)). Expression (5.29) is a polynomial in $e^{\pm Z_{\alpha_k}^h/2}$, $e^{\pm Z_j^h}$, ω_j and is clearly proportional to $e^{\pi_{j_1}^h/2} e^{\pi_{j_2}^h/2}$ with coefficients that are in turn Laurent polynomials of $q^{1/4}$ with positive integer coefficients. It is easy to see that expressing the terms of this operatorial expansion in terms of λ -lengths from the special $\text{CGL}_{\mathbf{a}}^{\max}$ using formulas (5.30)–(5.32) we have that every λ -length from this set enters every term of this expansion even number of times (every time in power $+1/2$ or $-1/2$) so the total power of any λ -length is necessarily integer in every term of expansion of (5.29), which completes the proof of the theorem.

Remark 5.1. Because the quantum geodesic function G_{γ} of every *closed* geodesic γ in $\Sigma_{g,s,n}$ is also a quantum polynomial in $e^{\pm Z_{\alpha}/2}$, $e^{\pm Z_j}$, ω_j , and $q^{\pm 1/2}$ with positive integer coefficients, this geodesic function can be again expressed as a Laurent polynomial in λ -lengths from a given $\text{CGL}_{\mathbf{a}}^{\max}$. λ -lengths thus indeed provide an alternative parameterization of the complete set of geodesic functions for $\Sigma_{g,s,n}$ with $n > 0$.

5.4.1. *Quantum mutations of quantum cluster variables.* For quantum arcs we have the following mutation rules:

- Mutating a general inner arc λ_e (neither a boundary arc nor an arc bounding a monogon) for the resulting quantum arc λ_f^h we obtain

$$(5.33) \quad \lambda_f^h = \lambda_a^h (\lambda_e^h)^{-1} \lambda_c^h + \lambda_b^h (\lambda_e^h)^{-1} \lambda_d^h \quad (\text{cf. Fig 3}).$$

Here all combinations of four bordered cusps can be identified (for instance, for $\Sigma_{g,s,1}$ all these cusps coincide and all arcs start and terminate at this single cusp), but for all these combinations we have that

$$\left(\lambda_a^h (\lambda_e^h)^{-1} \lambda_c^h \right)^* = \lambda_c^h (\lambda_e^h)^{-1} \lambda_a^h = \lambda_a^h (\lambda_e^h)^{-1} \lambda_c^h$$

and

$$\left(\lambda_b^h (\lambda_e^h)^{-1} \lambda_d^h \right)^* = \lambda_d^h (\lambda_e^h)^{-1} \lambda_b^h = \lambda_b^h (\lambda_e^h)^{-1} \lambda_d^h,$$

so formula (5.33) holds.

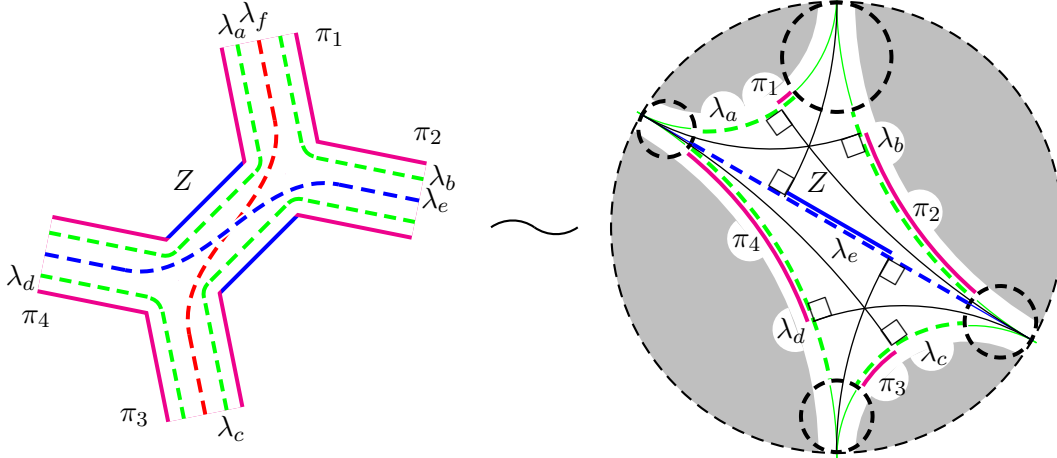


FIGURE 20. $\Sigma_{0,1,4}$ —a decorated ideal quadrangle. We indicate all five shear coordinates; four of them (π_i) correspond to external sides that constitute the boundary of a hole containing four bordered cusps decorated with horocycles, the fifth coordinate Z corresponds to the inner edge. In this example, the signed distance Z is negative. Dashed lines correspond to the λ -lengths, solid lines correspond to the shear coordinates.

- For a quantum arc λ_c^h that bounds a monogon, we have

$$(5.34) \quad \lambda_d^h = \lambda_a^h (\lambda_c^h)^{-1} \lambda_a^h + \lambda_b^h (\lambda_c^h)^{-1} \lambda_b^h + \omega_j q^{-I(a_a, a_c)/4 + I(a_b, a_c)/4} \lambda_a^h (\lambda_c^h)^{-1} \lambda_b^h \quad (\text{cf. Fig. 5}),$$

and whereas the first two summands in the right-hand side are obviously self adjoint, it is the only case of quantum mutations (for $\omega_j \neq 0$) where an explicit q -factor appears. Note that λ_a^h always commutes with λ_b^h and either $I(a_a, a_c) = I(a_b, a_c) = 0$ or one of these intersection indices vanishes and the other is equal to ± 4 , so possible powers of q in (5.34) are $-1, 0, 1$.

- No mutation of bordering arcs are allowed.

Example 5.2. We now consider in details the example of $\Sigma_{0,1,4}$ represented by an ideal quadrangle in Fig. 20. In this case, we have five shear coordinates: π_i , $i = 1, \dots, 4$ and Z and six arcs indicated by dashed lines in the left-hand side of the figure. The lambda lengths of all six possible arcs are

$$(5.35) \quad \begin{aligned} \lambda_a &= e^{\pi_1/2 + \pi_4/2 + Z/2}, & \lambda_b &= e^{\pi_1/2 + \pi_2/2}, & \lambda_c &= e^{\pi_2/2 + \pi_3/2 + Z/2}, \\ \lambda_d &= e^{\pi_3/2 + \pi_4/2}, & \lambda_e &= e^{\pi_2/2 + \pi_4/2 + Z/2}, & \lambda_f &= e^{\pi_1/2 + \pi_3/2 + Z/2} + e^{\pi_1/2 + \pi_3/2 - Z/2}, \end{aligned}$$

the nontrivial commutation relations are

$$(5.36) \quad [\pi_1, \pi_2] = [\pi_2, Z] = [Z, \pi_1] = [\pi_3, \pi_4] = [\pi_4, Z] = [Z, \pi_3] = 2\pi i \hbar,$$

and the only nonhomogeneous commutation relation is between λ_e and λ_f :

$$(5.37) \quad \lambda_e \lambda_f = q^{1/2} \lambda_a \lambda_c + q^{-1/2} \lambda_b \lambda_d; \quad \lambda_f \lambda_e = q^{-1/2} \lambda_a \lambda_c + q^{1/2} \lambda_b \lambda_d.$$

Example 5.3. Quantum cluster algebras associated with polygons—Riemann surfaces $\Sigma_{0,1,n}$ —are of finite type, as well as those associated with the “punctured” polygons—Riemann surfaces $\Sigma_{0,2,n}$ in which all cusps are associated with the same boundary component. Let us consider the example of a triangle with one hole inside (cf. Fig. 7 in [25]); we let $\lambda_{i,j}$ denote the quantum λ -lengths of bordering arcs (frozen variables) joining vertices i and j , we let $\hat{\lambda}_{i,j}$ denote the quantum λ -lengths of the (unique) inner arcs joining the same vertices, and $\tilde{\lambda}_{i,i}$ the quantum λ -length of the loop starting and terminating at the i th vertex and going around the inner hole. We have six different seeds in total

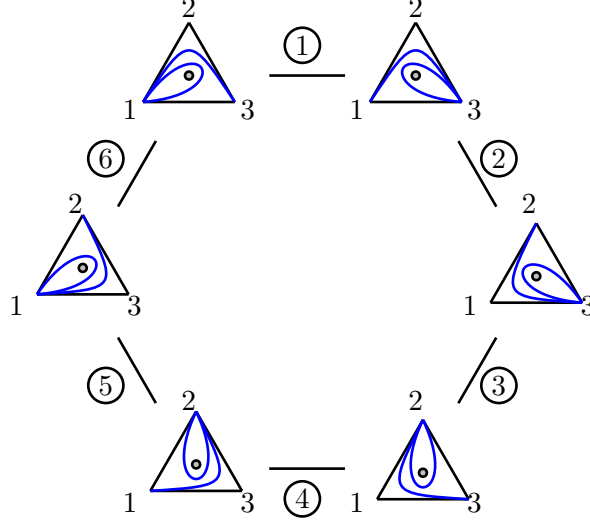


FIGURE 21. quantum cluster algebra structure for $\Sigma_{0,2,3}$ —triangle with the hole inside. We have six seeds related by six quantum mutations.

and they are related by six quantum mutations depicted in Fig. 21:

$$\begin{aligned}
 1: \quad & \tilde{\lambda}_{33} = \tilde{\lambda}_{13}(\tilde{\lambda}_{11})^{-1}\tilde{\lambda}_{13} + \omega\tilde{\lambda}_{13}\lambda_{13}(\tilde{\lambda}_{11})^{-1} + \lambda_{13}(\tilde{\lambda}_{11})^{-1}\lambda_{13}, \\
 2: \quad & \tilde{\lambda}_{23} = q^{1/4}\tilde{\lambda}_{33}\lambda_{12}(\tilde{\lambda}_{13})^{-1} + \lambda_{13}(\tilde{\lambda}_{13})^{-1}\lambda_{23}, \\
 3: \quad & \tilde{\lambda}_{22} = \tilde{\lambda}_{23}(\tilde{\lambda}_{33})^{-1}\tilde{\lambda}_{23} + \omega\tilde{\lambda}_{23}\lambda_{23}(\tilde{\lambda}_{33})^{-1} + \lambda_{23}(\tilde{\lambda}_{33})^{-1}\lambda_{23}, \\
 4: \quad & \tilde{\lambda}_{12} = q^{1/4}\tilde{\lambda}_{22}\lambda_{13}(\tilde{\lambda}_{23})^{-1} + \lambda_{23}(\tilde{\lambda}_{23})^{-1}\lambda_{12}, \\
 5: \quad & \tilde{\lambda}_{11} = \tilde{\lambda}_{12}(\tilde{\lambda}_{22})^{-1}\tilde{\lambda}_{12} + \omega\tilde{\lambda}_{12}\lambda_{12}(\tilde{\lambda}_{22})^{-1} + \lambda_{12}(\tilde{\lambda}_{22})^{-1}\lambda_{12}, \\
 6: \quad & \tilde{\lambda}_{12} = q^{1/4}\tilde{\lambda}_{11}\lambda_{23}(\tilde{\lambda}_{12})^{-1} + \lambda_{12}(\tilde{\lambda}_{12})^{-1}\lambda_{13}.
 \end{aligned}$$

6. CONCLUSION

We first recall the main new results obtained in this paper. We have developed a procedure that allows passing from Riemann surfaces with holes to Riemann surfaces with bordered cusps by colliding holes of the original Riemann surface. We gave a quantitative description of the newly obtained Riemann surfaces with decorated bordered cusps in terms of the extended shear coordinates and derived explicit combinatorial formulas for geodesic functions of closed geodesics and λ -lengths of arcs—geodesics stretched between decorated bordered cusps in terms of the extended shear coordinates. We postulate the Poisson and quantum commutation relations on the set of extended shear coordinates that are MCG invariant and generate the Goldman brackets on the set of geodesic and arc functions. For generalized laminations ([42], [41]) comprising both closed curves and arcs, we have found that maximum systems of arcs CGL_a^{\max} are quantum tori: their items (corresponding to compatible regular arcs in the terminology of [24]) have homogeneous commutation relations, transform in accordance with generalized mutation rules (see [14]) for quantum cluster algebras of Berenstein and Zelevinsky and can be therefore identified with seeds of these quantum cluster algebras. We have also found the explicit quantum ordering for quantum arcs proving that thus ordered expressions satisfy quantum skein relations.

In the forthcoming paper [11] we shall use the quantum ordering results of this paper for deriving explicit quantum algebras of monodromy matrices for the general n -point SL_2 Schlesinger system [15], [16]. It is also tempting to transfer our approach to quantum cluster algebras to quiver algebras of geometric origin studied in [44].

An interesting example of generalised cluster algebras has appeared recently in the paper by Gekhtman, Shapiro, and Vainshtein [30] where the authors constructed log-canonical (or Darboux) coordinates for GL_n algebras and demonstrated that they transform under the generalised cluster mutations. It is tempting to compare our approach with that of [30].

Results of this paper were first reported by the first named author on the Nielsen Retreat of QGM, Århus University, 26-29 October 2014. Simultaneously, the papers [22] and [1] had appeared dealing with similar issues. In particular, Allegretti had also introduced additional shear-type variables associated to external edges of an ideal triangle decomposition of a bordered cusped Riemann surfaces and observed (Lemma 6.3 in [1]) the monoidal relation between exponentiated shear coordinates and λ -lengths. However, neither Poisson nor quantum algebras of arc functions were considered there.

Acknowledgments. The authors wish to thank Volodya Rubtsov for several enlightening conversations on the main constructions of the paper. The authors are also grateful to Misha Shapiro and Anton Zeitlin for the useful discussion. The results of Sections 2 and 5 were obtained by L. Chekhov and the results of Sections 3 and 4 were obtained by M. Mazzocco. The work of L. O. Chekhov (the results of Sections 2 and 5) was supported by the Russian Science Foundation under grant 14-50-00005 and was performed in the Steklov Mathematical Institute of Russian Academy of Sciences.

REFERENCES

- [1] D. Allegretti, *Laminations from the symplectic double*, arXiv:1410.3035v1, 64 pp.
- [2] A. Berenstein and A. Zelevinsky, *Quantum cluster algebras* *Advances Math.* **195** (2005) 405–455; math/0404446.
- [3] F. Bonahon, *Shearing hyperbolic surfaces, bending pleated surfaces and Thurston’s symplectic form*, *Ann. Fac. Sci. Toulouse Math* **6** **5** (1996), 233–297.
- [4] Chekhov L. O., *Riemann surfaces with orbifold point*, *Proc. Steklov Math. Inst.*, **266** (2009), pp.1-26
- [5] Chekhov L. O., *Orbifold Riemann surfaces and geodesic algebras*, *J. Phys. A: Math. Theor.* **42** (2009) Paper 304007, 32 pp. (electronic)
- [6] Chekhov L., Fock V., *A quantum Teichmüller space*, *Theor. Math. Phys.* **120** (1999), 1245–1259, math.QA/9908165.
- [7] Chekhov L., Fock V., *Quantum mapping class group, pentagon relation, and geodesics*, *Proc. Steklov Math. Inst.* **226** (1999), 149–163.
- [8] Chekhov L.O., Mazzocco M., *Isomonodromic deformations and twisted Yangians arising in Teichmüller theory*, *Advances Math.* **226**(6) (2011) 4731–4775, arXiv:0909.5350.
- [9] L.O. Chekhov, M. Mazzocco, *Shear coordinate description of the quantized versal unfolding of a D_4 singularity* *J. Phys. A: Math. Theor.* **43** (2010) 442002 (9pp.)
- [10] Chekhov L.O. and Mazzocco M., *Quantum ordering for quantum geodesic functions of orbifold Riemann surfaces*, *Amer. Math. Soc. Translations–Ser. 2* **234** (2014) 93–116, arXiv:1309.3493.
- [11] Chekhov L.O. and Mazzocco M., *Quantum algebras of monodromies for SL_2 Schlesinger systems* (in preparation).
- [12] Chekhov L., Mazzocco M., Rubtsov V., *Painlevé monodromy manifolds, decorated character varieties and cluster algebras*, arXiv:1511.03851.
- [13] L.O. Chekhov and R.C. Penner, *Introduction to quantum Thurston theory*, *Russ. Math. Surv.* **58**(6) (2003) 1141–1183.
- [14] L. Chekhov and M. Shapiro *Teichmüller spaces of Riemann surfaces with orbifold points of arbitrary order and cluster variables*, *Intl. Math. Res. Notices* 2013; doi: 10.1093/imrn/rnt016. (arXiv:1111.3963, 20pp)
- [15] Dubrovin B., *Geometry of 2D topological field theories, Integrable systems and quantum groups* (Montecatini Terme, 1993), *Lecture Notes in Math.*, **1620**, Springer, Berlin, (1996) 120–348.
- [16] Dubrovin B.A., Mazzocco M., *Monodromy of certain Painlevé-VI transcendents and reflection group*, *Invent. Math.* **141** (2000), 55–147.
- [17] L. D. Faddeev and R. M. Kashaev, *Quantum dilogarithm*, *Modern Phys. Lett.* **A9** (1994) 427–434, hep-th/9310070.
- [18] L. D. Faddeev, *Discrete Heisenberg–Weyl group and modular group*, *Lett. Math. Phys.*, **34**, (1995), 249–254.
- [19] Fock V.V., *Combinatorial description of the moduli space of projective structures*, hep-th/9312193.
- [20] V. V. Fock and A. B. Goncharov, *Moduli spaces of local systems and higher Teichmüller theory*, *Publ. Math. Inst. Hautes Études Sci.* **103** (2006), 1–211, math.AG/0311149 v4.
- [21] V. V. Fock and A. B. Goncharov, *Dual Teichmüller and lamination spaces*, Chapter 15 in: *Handbook on Teichmüller Theory*, Vol.1 (IRMA Lectures in Mathematics and Physics, Vol.11), ed. A. Papadopoulos, IRMA Publ., Strasbourg, France. pp.647–684; math.DG/0510312.
- [22] V. Fock and A. Goncharov, *Symplectic double for moduli spaces of G -local systems on surfaces* (2014) arXiv:1410.3526, 37pp.

- [23] V. V. Fock and A. A. Rosly, *Moduli space of flat connections as a Poisson manifold*, *Internat. J. Modern Phys. B* **11** (1997), no. 26-27, 3195–3206.
- [24] Fomin S. and Thurston D., *Cluster algebras and triangulated surfaces. Part II: Lambda lengths*, arXiv:1210.5569.
- [25] Fomin S., Shapiro M., and Thurston D., *Cluster algebras and triangulated surfaces. Part I: Cluster complexes*, *Acta Math.* **201** (2008), no. 1, 83–146.
- [26] S. Fomin and A. Zelevinsky, *Cluster algebras I: Foundations*, *J. Amer. Math. Soc.* **15**(2) (2002) 497–529.
- [27] S. Fomin and A. Zelevinsky, *The Laurent phenomenon*, *Adv. in Appl. Math.* **28** (2002), no. 2, 119–144.
- [28] S. Fomin and A. Zelevinsky, *Cluster algebra II: : Finite type classification* *Invent. Math.*, **154** (2003), no. 1, 63–121.
- [29] M. Gekhtman, M. Shapiro, and A. Vainshtein, *Cluster algebra and Poisson geometry*, *Moscow Math. J.* **3**(3) (2003) 899–934.
- [30] M. Gekhtman, M. Shapiro, and A. Vainshtein, *Generalized cluster structure on the Drinfeld double of GL_n* , arXiv:1507.00452.
- [31] Goldman W.M., *Invariant functions on Lie groups and Hamiltonian flows of surface group representations*, *Invent. Math.* **85** (1986), 263–302.
- [32] R. M. Kashaev, *Quantization of Teichmüller spaces and the quantum dilogarithm*, *Lett. Math. Phys.* **43**(1998), 105–115, q-alg/9706018.
- [33] R. M. Kashaev, *On the spectrum of Dehn twists in quantum Teichmüller theory*, in: *Physics and Combinatorics*, (Nagoya 2000). River Edge, NJ, World Sci. Publ., 2001, 63–81; math.QA/0008148.
- [34] R. M. Kaufmann and R. C. Penner, *Closed/open string diagrammatics*, *Nucl. Phys.* **B748** (2006) 335–379.
- [35] P. P. Kulish and E. K. Sklyanin, *Quantum spectral transform method: Recent developments*, in *Integrable Quantum Field Theories* (Lect. Notes in Physics,: Vol. 151), Berlin, Springer, 1982, pp. 61–119.
- [36] Mazzocco M., *Confluences of the Painlevé equations, Cherednik algebras and q-Askey scheme*, arXiv:1307.6140.
- [37] Molev A., *Yangians and classical Lie algebras. Mathematical Surveys and Monographs*, **143**, American Mathematical Society, Providence, RI, (2007).
- [38] A. Molev, E. Ragoucy, *Symmetries and invariants of twisted quantum algebras and associated Poisson algebras*, *Rev. Math. Phys.*, **20**(2) (2008) 173–198.
- [39] A. Molev, E. Ragoucy, P. Sorba, *Coideal subalgebras in quantum affine algebras*, *Rev. Math. Phys.*, **15** (2003) 789–822.
- [40] G. Musiker, R. Schiffler, and L. Williams, *Positivity for cluster algebras from surfaces*, *Adv. Math.*, **227**(6) (2011) 2241–2308.
- [41] G. Musiker, R. Schiffler, and L. Williams, *Bases for cluster algebras from surfaces*, *Compositio Math.*, **149**(2) (2013) 217–263; arXiv:1110.4364.
- [42] G. Musiker and L. Williams, *Matrix formulae and skein relations for cluster algebras from surfaces* *Intl. Math. Res. Notices* **2013**(13) (2013) 2891–2944.
- [43] M. L. Nazarov, *Quantum Berezinian and the classical Capelli identity*, *Lett. Math. Phys.* **21** (1991) 123–131.
- [44] D. Orlov, *Geometric realisations of quiver algebras* *Proc. Steklov Inst. Math.* **290** (2015) 70–83; arXiv:1503.03174.
- [45] Penner R.C., *The decorated Teichmüller space of Riemann surfaces*, *Comm. Math. Phys.* **113** (1988), 299–339.
- [46] W. P. Thurston, *Minimal stretch maps between hyperbolic surfaces*, preprint (1984), math.GT/9801039.